# SEDIMENT LOGS COMPILED FROM THE GREAT SALT LAKE DESERT, WESTERN UTAH, WITH A FOCUS ON THE BONNEVILLE SALT FLATS AREA

*by Jeremiah A. Bernau, Charles G. Oviatt, Donald L. Clark, and Brenda B. Bowen*

**OPEN-FILE REPORT 754**
**UTAH GEOLOGICAL SURVEY**
UTAH DEPARTMENT OF NATURAL RESOURCES
**2023**

*Blank pages are intentional for printing purposes.*

# SEDIMENT LOGS COMPILED FROM THE GREAT SALT LAKE DESERT, WESTERN UTAH, WITH A FOCUS ON THE BONNEVILLE SALT FLATS AREA

*by*


*Jeremiah A. Bernau[1], Charles G. Oviatt[2], Donald L. Clark[1], and Brenda B. Bowen[3]*

*[1]Utah Geological Survey, Salt Lake City, Utah*

*[2]Emeritus, Department of Geology, Kansas State University, Manhattan, Kansas*

*[3]Director, Global Change and Sustainability Center, Professor, University of Utah, Department of Geology & Geophysics, Salt Lake City, Utah*


***Cover photo:*** *Silver Island Mountains alluvial fan-mudflat interface, looking northwest. The change in elevation and vegetation between the alluvial fan and mudflat is interpreted as the result of the local deflation of Lake Bonneville sediments. Photo by Jeremiah Bernau.*


Suggested citation:

Bernau, J.A., Oviatt, C.G., Clark, D.L. and Bowen, B.B., 2023, Sediment logs compiled from the Great Salt Lake Desert, western Utah, with a focus on the Bonneville Salt Flats area: Utah Geological Survey Open-File Report 754, 24 p., 3 appendices, https://doi.org/10.34191/OFR-754.

**OPEN-FILE REPORT 754**
**UTAH GEOLOGICAL SURVEY**
UTAH DEPARTMENT OF NATURAL RESOURCES
**2023**

**STATE OF UTAH**
Spencer J. Cox, Governor

**DEPARTMENT OF NATURAL RESOURCES**
Joel Ferry, Executive Director

**UTAH GEOLOGICAL SURVEY**
R. William Keach II, Director

**PUBLICATIONS**
contact
Natural Resources Map & Bookstore
1594 W. North Temple
Salt Lake City, UT 84116
telephone: 801-537-3320
toll-free: 1-888-UTAH MAP
website: utahmapstore.com
email: geostore@utah.gov

**UTAH GEOLOGICAL SURVEY**
contact
1594 W. North Temple, Suite 3110
Salt Lake City, UT 84116
telephone: 801-537-3300
website: geology.utah.gov



*This project was partially funded by the Utah Geological Survey, U.S. Geological Survey, University of Utah, and National Science Foundation (Award #1617473). The views and conclusions contained in this document are those of the authors and should not be interpreted as necessarily representing the official policies, either expressed or implied, of the U.S. Government.*

# CONTENTS



# FIGURES

## TABLES

# INTRODUCTION

This document presents a compilation of previously published sediment logs and unpublished water well logs from the Bonneville Salt Flats area, and reports new data from several trench exposures. Furthermore, we report additional smear slide and ostracode observations from a subset of previously described shallow sediment cores and exposures (Oviatt and others, 2020). This dataset is associated with ongoing Utah Geological Survey (UGS) work on the evaluation of groundwater, geologic history, and geologic mapping (Clark and others, 2020; in preparation) in the vicinity of the Bonneville Salt Flats. Part of this work was conducted by Bernau as a part of his Ph.D. research.

Sediment logs from exposures, excavations, cores, and wells are valuable records that can be used to interpret depositional records, aquifer extents, and geologic structures. Here we present sediment logs compiled from the Great Salt Lake Desert (GSLD) in western Utah with a specific focus on the Bonneville Salt Flats area. The logs are grouped into three categories (shallow, alluvial fan, and deep) that may be used to explore different aspects of GSLD deposition (figure 1).

The first group, shallow logs (<15 m deep, 3.3 m on average), contains Holocene to late Pleistocene depositional records that may be used to understand GSLD depositional and deflationary trends. The thicknesses of Holocene sediments are summarized in table 1. Underlying Lake Bonneville sediments were examined and delineated by presence, stratigraphic completeness, and thickness of Lake Bonneville strata.

The second group, alluvial-fan logs, consists of deeper (32–111 m deep, 64 m on average) well and sediment log data from the eastern-facing sides of the southwest Silver Island Mountains and southeast of the Leppy Hills area. These logs intersect an alluvial-fan aquifer that is of particular interest to understanding ongoing change in volume and area of salt crust at the Bonneville Salt Flats, a dynamic landscape valued for potash production, scientific interest, vehicular land-speed racing, and other recreation (e.g., Bingham, 1980; Bowen and others, 2018a).

The third group, deep logs (450 m deep on average), consists of logs from wells drilled for scientific, petroleum, and mineral extraction purposes (Shuey, 1971; Turk, 1973; Stephens, 1974). These logs shed insights into this region's changing depositional history, the distribution of a deep brine aquifer used for potash production, and provides constraints on the Wendover graben in the western GSLD.

# METHODS

We used several programs to visualize data and collected new data from several sites. The PSICAT program, a tool for logging and visualizing macroscopic features (Reed, 2007), was used to generate sediment logs. Additional smear slide and ostracode analyses were performed on a subset of samples. Mineralogy, ostracode fragment, diatom, and diatom cyst (chrysophyte) presence was determined with smear slide analysis (Schnurrenberger and others, 2003). Sediment samples were processed to determine the presence or absence of rod-shaped carbonate pellets (brine-shrimp fecal pellet ooids) and ostracode presence and genera/species through visual inspection under a microscope. Using a modification of Forester's (1988) ostracode preparation methodology (without the sample freezing step), we treated sediment samples with warmed deionized water and then wet sieved them. We analyzed the 106–250 µm fraction. Oviatt identified the ostracode genera/species. Visualizations of smear slides and ostracode data were generated using the R programming environment (R Core Team, 2021). Our smear slide and ostracode data are shown in appendix A. Sediment log data is available in tabular form in appendix B. Sediment log data is visualized in appendix C.

In addition to compiling sediment log information, we created maps visualizing this information in ArcGIS Pro. As part of this data visualization, we generated contour maps of select strata using the natural neighbor interpolation method.

# DATASETS AND PREVIOUS WORK

## Shallow Logs

Shallow logs were examined to determine the thickness of Holocene deposits and the presence, thickness, and stratigraphic completeness of underlying Lake Bonneville sediments. We identified Lake Bonneville sediments by radiocarbon

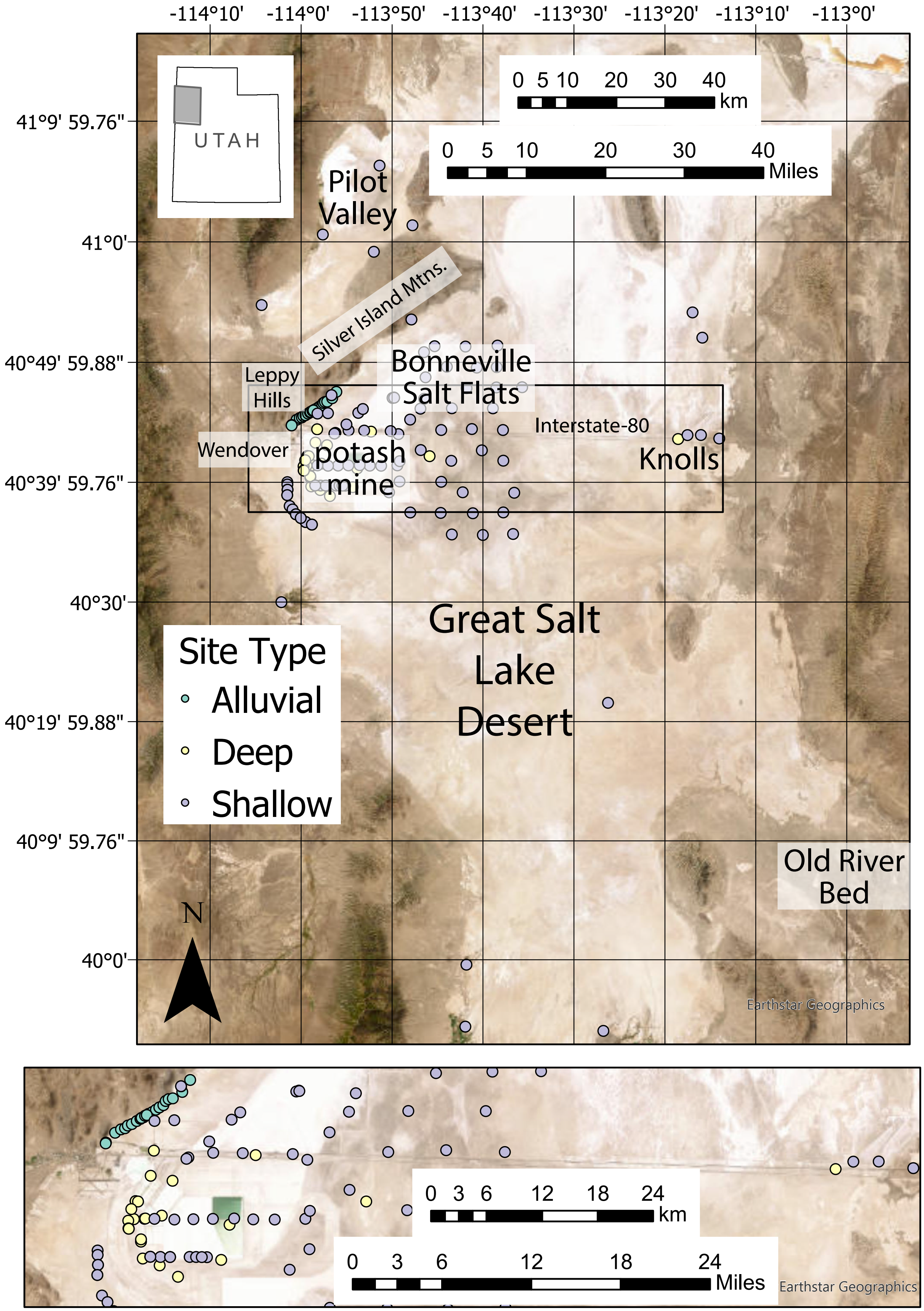


***Figure 1.*** *Overview of shallow, alluvial-fan, and deep sites. Inset in the upper part of the figure shown at figure base.*

dating, ostracode genera/species assemblage, and sedimentological characteristics. Where sufficient data were available, we interpreted three Lake Bonneville stratigraphic units: Provo/post-Bonneville flood marl (PM), massive marl (MM), and laminated marl (LM). This stratigraphic differentiation has been used in several areas across the Lake Bonneville basin (Oviatt and others, 1994; Rey and others, 2016; Oviatt and others, 2018; Oviatt, 2021) and the chronology is as follows: PM (13–18 cal ka), MM (18–24 cal ka), and LM (24–30 cal ka) (figure 2).

Nolan (1927), as part of his investigation of brine resources, was one of the earliest known researchers to document the shallow stratigraphy of the GSLD. The Bonneville Salt Flats have been the site of sediment examination several times since the 1960s to determine changes in salt crust thickness over time (e.g., Bowen and others, 2018b; Kipnis and Bowen, 2018). The most recent salt crust thickness study showed that the Bonneville Salt Flats' evaporite crust consists of an elongated lens-shaped deposit that is ~1.5 m thick at its center and thins to zero at the edges (Bowen and others, 2018b). We describe a subset of stratigraphically constrained cores from the Bonneville Salt Flats here but do not discuss this larger dataset of shallow cores further. The shallow sediment logs we describe are summarized in table 1 and displayed in figure 3. The thickness of Holocene deposits and the presence, thickness, and stratigraphic completeness of underlying Lake Bonneville sediments in shallow logs are displayed in figures 4 to 6.

Additional logs that we did not incorporate into this report are a 20-m-deep log with cone penetrometer data collected near Knolls, Utah, as part of a seismic study (Badri and Mooney, 1987), and non-Bonneville Salt Flats-area shallow logs in the water rights database (Utah Division of Water Rights, 2022). Surficial deposits in the Great Salt Lake are shown in geologic map publications (Clark and others, 2016; Clark and others, 2020; Miller and others, 2021; Clark and others, in preparation).

## Previous Work

**Grim and others, 1960; Graf and others, 1961; Bissell and Chilingar, 1962; Eardley, 1962:** Several shallow cores were collected on an east-west transect in GSLD in the late 1950s to early 1960s (Grim and others, 1960; Graf and others, 1961; Eardley, 1962). These cores were examined for clay (Grim and others, 1960) and carbonate mineralogy (Graf and others, 1961; Bissell and Chilingar, 1962).

In addition to describing the larger east-west transect of shallow GSLD cores, Eardley (1962) described three pits and several sites along a potash mine trench exposure. Sediments from the pits were dated using radiocarbon. We used our stratigraphic observations of other potash mine ditches to make preliminary stratigraphic interpretations of Eardley's trench exposure.

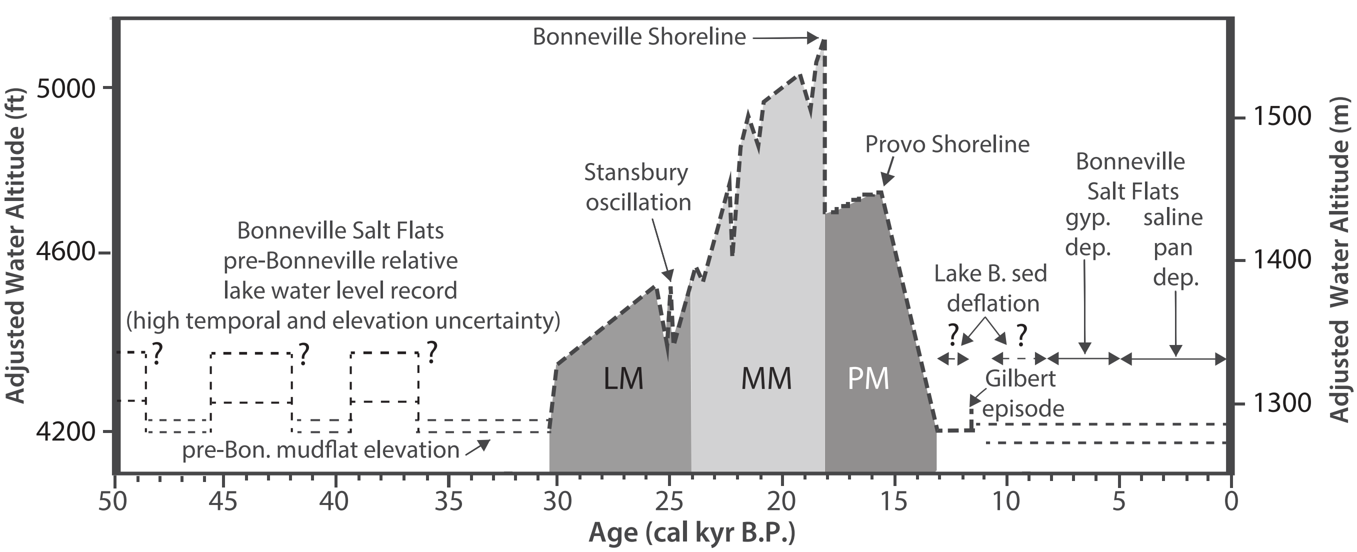


***Figure 2.*** *Regional hydrograph for post-Lake Bonneville, Lake Bonneville, and pre-Bonneville conditions in the Great Salt Lake Desert based on regional records and records from the Bonneville Salt Flats (Bernau and others, in review). Note different lake stages and associated sediment types: Provo and post-Bonneville flood marls (PM), massive marl (MM), or early Lake Bonneville laminated marls (LM). Lake Bonneville hydrograph is modified from Oviatt (2015).*

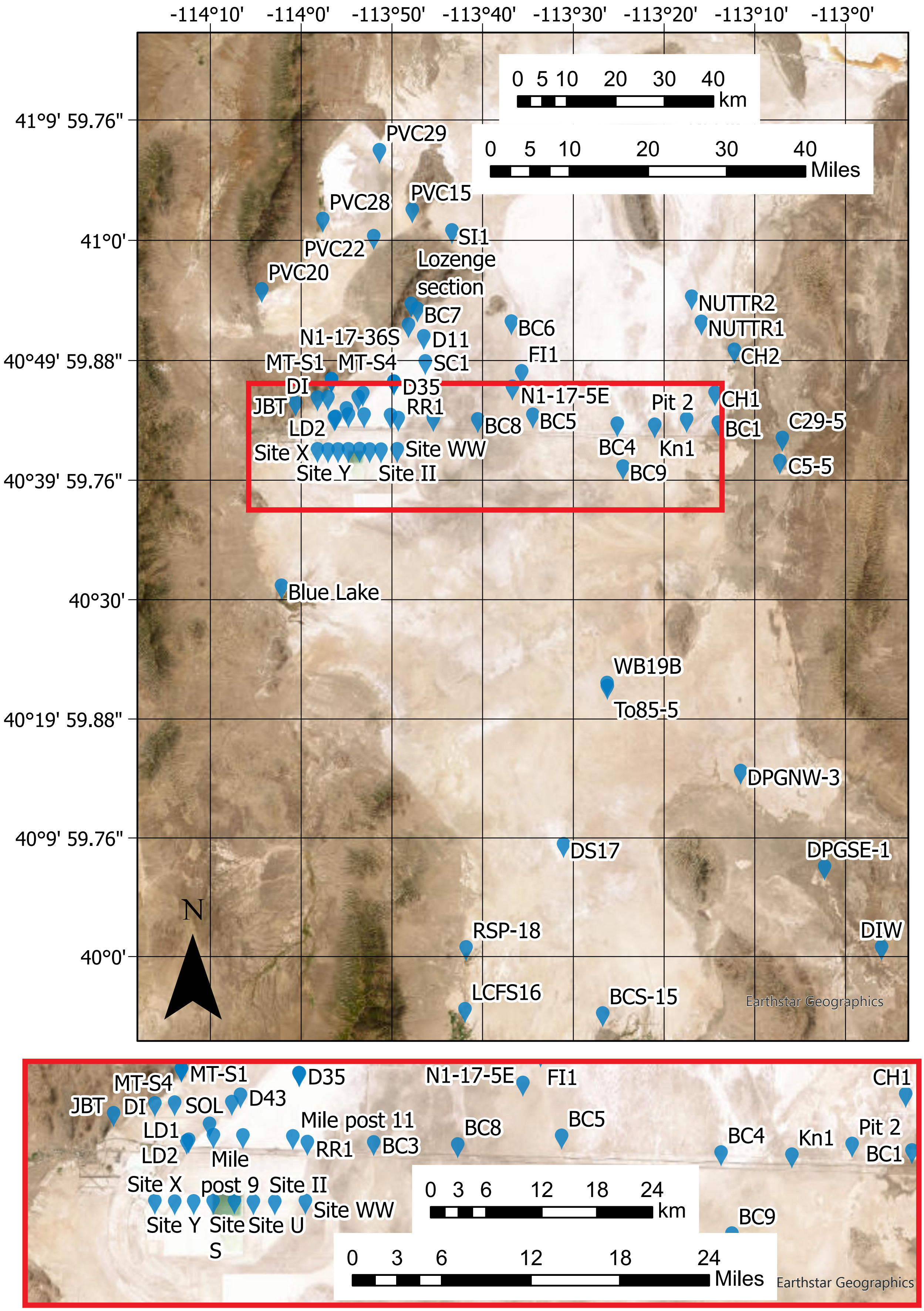


***Figure 3.*** *Locations and IDs of shallow sites. Note: only sites from figure 1 having some stratigraphic constraints are shown.*

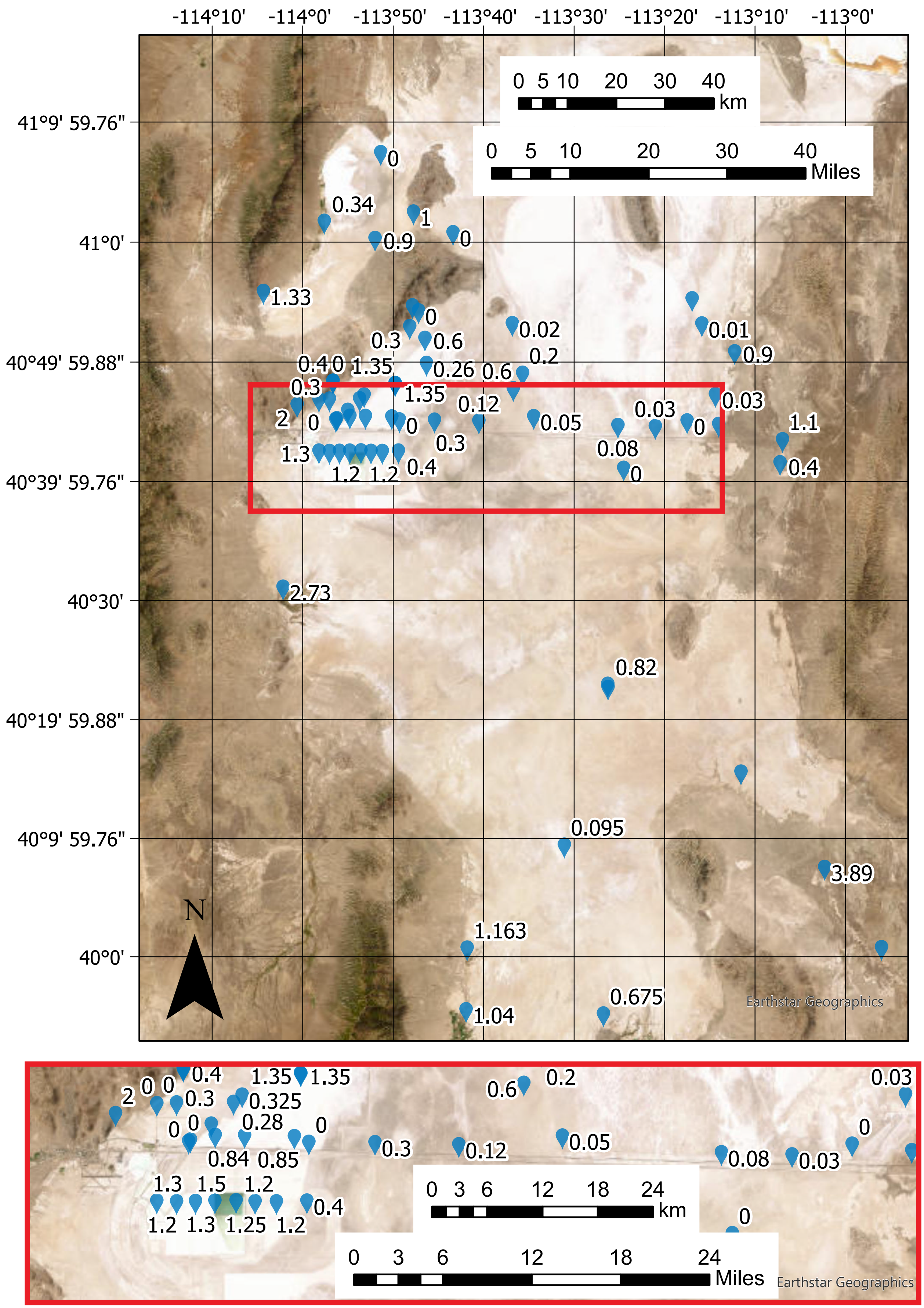


*Figure 4. Post-Lake Bonneville Holocene to late Pleistocene depositional thickness (m) at the shallow sites.*

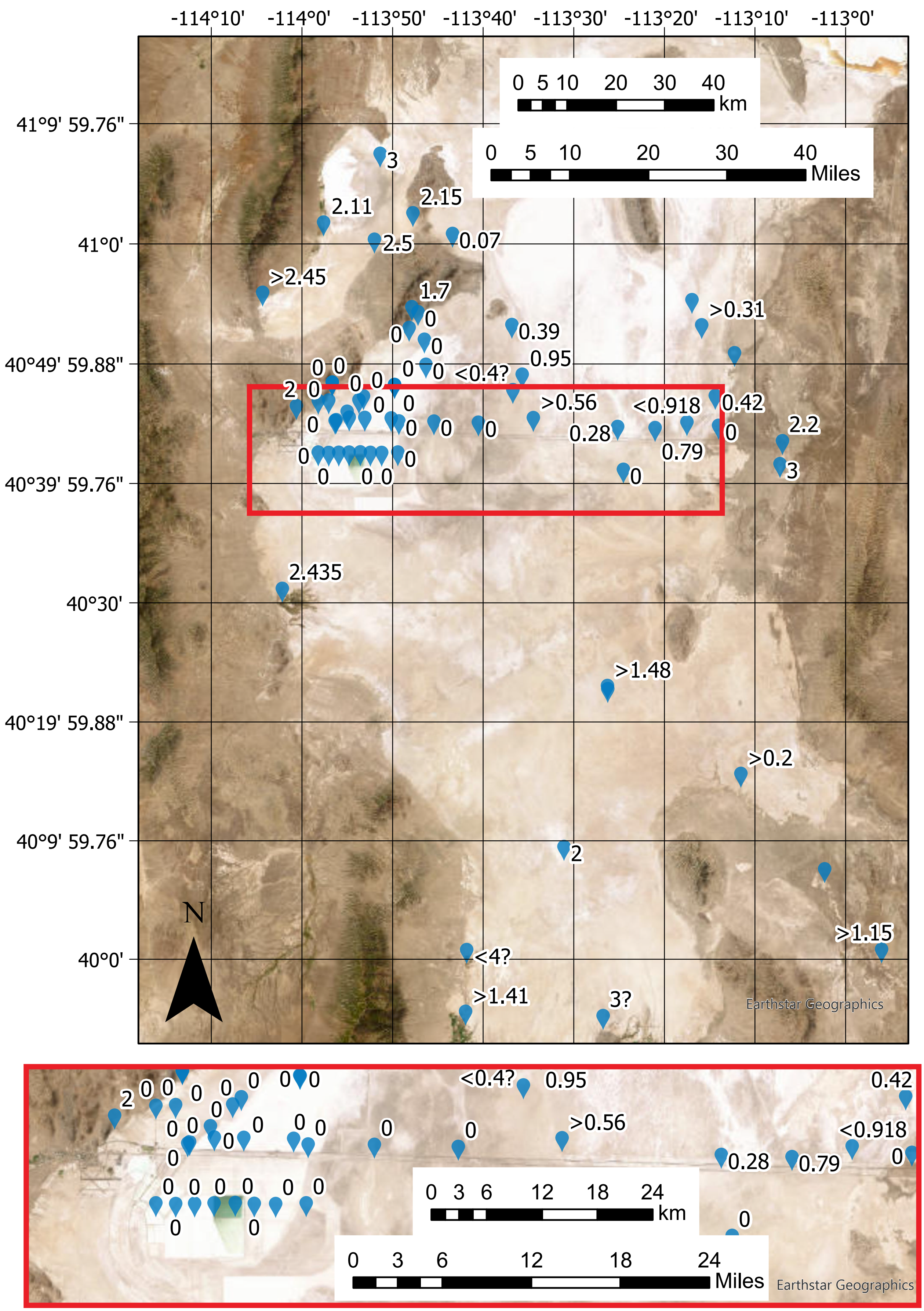


***Figure 5.*** *Thickness (m) of Lake Bonneville sediments at the shallow sites.*

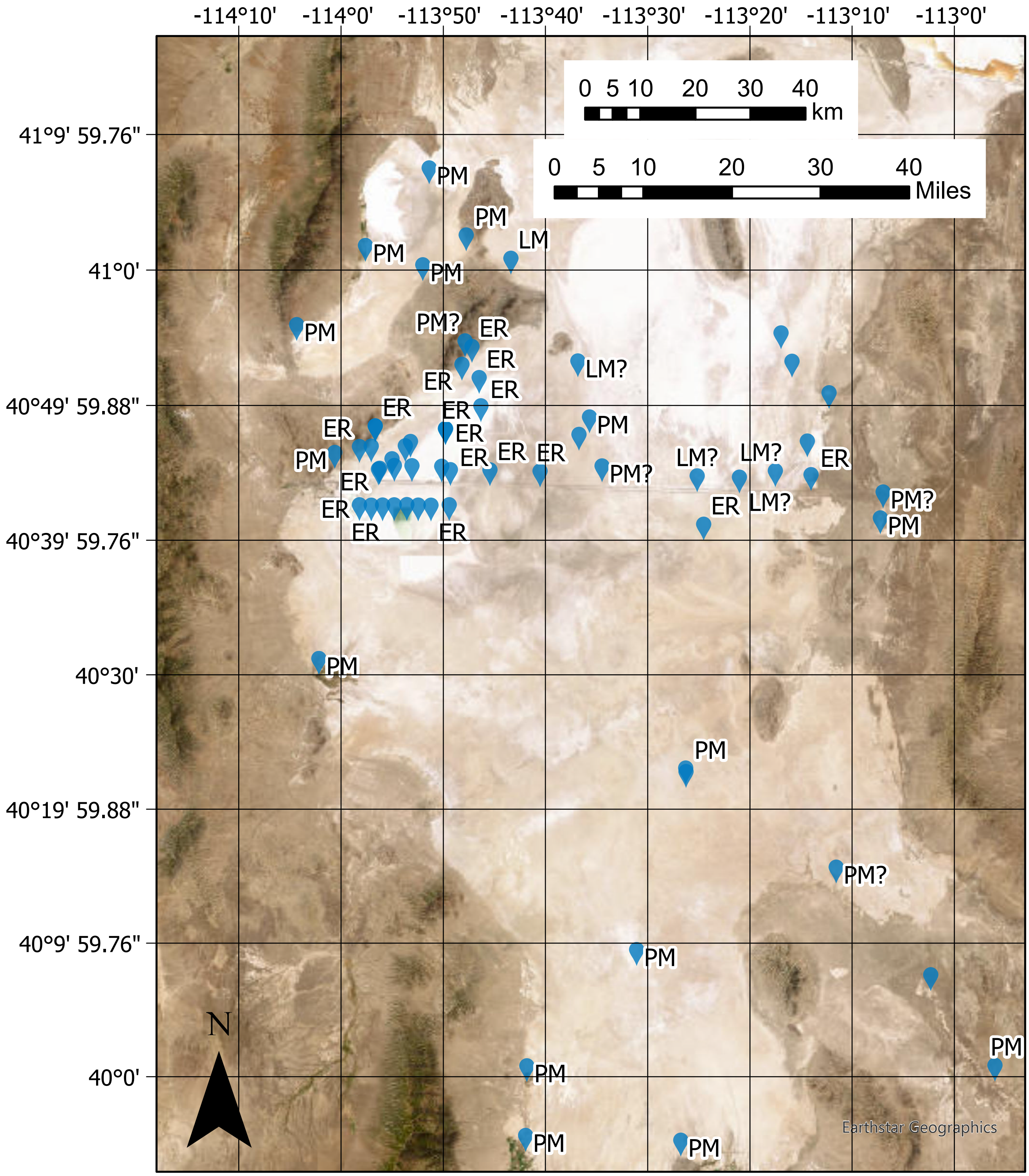


***Figure 6.*** *Lithology type of the topmost identified Lake Bonneville sediments in shallow sediment sites denoted by "PM" for Provo and post-Bonneville flood marl, "MM" for massive marl, "LM" for laminated marl, or "ER" if eroded.*

**Nackowski, 1962:** Nackowski (1962) collected 34 shallow (4.5–4.9 m) sediment logs across and to the east of the Bonneville Salt Flats and potash mine as part of a potash exploration program. The sediment logs include grain size, color, moisture percent, water level, and macroscopic sedimentary features.

**Neilsen and others, 1962:** Neilsen and others (1962) excavated cores across GSLD in preparation for the construction of Interstate Highway 80. They reported the lithology and engineering characteristics of three ~14-m-deep cores collected along the Bonneville Salt Flats. Without data from nearby sites, these logs are of limited value.

**Turk, 1973:** Turk (1973) described two different exposures along trenches in the potash mine. Turk's descriptions, although showing variability in bed thickness, are only lithological, limiting stratigraphic interpretation. We made preliminary stratigraphic interpretations of sediments based on our analysis of nearby shallow sediment logs.

**Lindenburg, 1974:** Lindenburg (1974) collected shallow brines from GSLD and reported two sediment logs in his thesis. We made preliminary stratigraphic interpretations of sediments based on these descriptions and our analysis of nearby shallow sediment logs.

**Oviatt and others, 2003:** Oviatt and others (2003) described early Holocene to late Pleistocene fluvial and wetland deposits in the Old River Bed near Dugway, Utah. Two sites were described in detail and are reported here.

**Fitzmayer and others, 2004:** Fitzmayer and others (2004) described the hydrogeology of the Government Creek Basin in Dugway, Utah. Their report included a 91 m generalized stratigraphic description and refers to over 200 monitoring wells installed in this area. However, no primary data was reported.

**Rey, 2012; Rey and others, 2016; and Mayo and others, 2020:** Rey (2012) and Rey and others (2016) described shallow cores collected across the GSLD Pilot Valley embayment. These cores were characterized by lithology, constrained with radiocarbon dating, and by ostracode genera/species occurrence. The identified units correlate with Lake Bonneville stratigraphy of PM, MM, LM, and pre-and post-Lake Bonneville sediments. The elevation of the top of PM, MM, and pre-Bonneville sediments from these cores was mapped by Mayo and others (2020).

**Madsen and others, 2015:** Madsen and others (2015) described over two dozen Old River Bed delta sites in detail with a focus on early Holocene to late Pleistocene stratigraphy. The description of those sites is beyond our scope of interest and is not further described here.

**Pedone and Oviatt, 2013 and 2016:** Pedone and Oviatt (2013 and 2016) described GSLD shallow cores for their total inorganic carbon, strontium and carbonate stable isotope ratios, and aragonite and calcite ratios. The Bonneville flood (~18 cal ka) and post-Stansbury oscillation (~24 cal ka) were interpreted.

**Oviatt and others, 2020:** Our report builds on the shallow sediment log dataset published by Oviatt and others (2020). Their publication described new sites and compiled data and new interpretations from previously described sites (Williams, 1994; Louderback and Rhode, 2009; Benson and others, 2011; Munroe and others, 2015; Oviatt, 2017; Oviatt and others, 2018). New measurements in that report primarily focused on ostracode genera/species occurrence. Oviatt and others (2020) identified the absence of Lake Bonneville sediments at the Bonneville Salt Flats and the surrounding area.

**Palacios-Fest and others, 2021:** Palacios-Fest and others (2021) described 11 sites, with a focus on the Old River Bed area. They examined and dated post-Lake Bonneville material and described evidence of post-Lake Bonneville freshwater lake deposits that unconformably overlie Lake Bonneville deposits. Detailed stratigraphy of only one site (To85-5), with five interpreted units, was available and is reported here.

**Hart and others, 2022:** Hart and others (2022) reported radiocarbon-based age-depth model ages of several cores from the southern GSLD. These cores were correlated with portable X-ray fluorescence spectrometer measurements and visual alignment of stratigraphic intervals.

**Bernau, 2022, and Bernau and others, in review:** Bernau (2022) and Bernau and others (in review) described smear slide mineralogical data and ostracode abundance data in three cores from the Bonneville Salt Flats that were previously described in Oviatt and others (2020). Radiocarbon dating with an age-depth model and ostracode occurrence was used to constrain the depositional timing of interpreted strata. We use Bernau and others' (in review) pre-Bonneville stratigraphic units to interpret a portion of sediment logs (figure 7 and appendix C).

**This work:** We describe four new sediment log sites based on measurements and samples collected from ditch exposures in the area surrounding the Bonneville Salt Flats (DI, LD1 and LD2, MT-S1 and MT-S4, and RR1) (table 1). Sites LD1, LD2, and RR1 were located in potash mine ditches. The DI, MT-S1, and MT-S4 sites were located to the west of the Bonneville Salt Flats. The DI site was in a ditch used to transport alluvial-fan water to the potash mine and the MT-S1 and MT-S4 sites were in a trench excavated in a former spring-fed wetland area.

In addition to these new sites, we also collected additional ostracode and smear slide samples from some sites described in Oviatt and others (2020) and two cores from the 2016 salt crust thickness study (Bowen and others, 2018b) (D11 and D43). This information is reported in appendix A.

## Depositional Trends

An east-west transect of a subset of shallow cores with interpreted strata added shows ~1 to 3 m of post-Bonneville, Holocene to late Pleistocene deposition occurring on the edges of the basin floor (figure 7). Higher Holocene to late Pleistocene depositional rates at basin floor edges correspond with springs on GSLD's western edge, eolian deposition on the GSLD's eastern edge, and Old River Bed fluvial deposits in the southeastern GSLD. Holocene to late Pleistocene deposition on the basin floor is concentrated at the Bonneville Salt Flats and eolian dunes, such as those at Knolls. Lake Bonneville sediments are thicker at the edges of GSLD. In the basin floor, Lake Bonneville sediments are absent in the area surrounding the Bonneville Salt Flats. Lake Bonneville sediments may be absent in some areas on the eastern edge of GSLD as they were not clearly identifiable in cores BC9 and BC1. Lake Bonneville sediments are partially eroded in most areas between Knolls dunes and the Bonneville Salt Flats. We created a chronostratigraphic diagram of preserved deposits over time (figure 8) based on the interpreted age of sediments in the east-west transect (figure 7).

## Alluvial-Fan Logs

Several alluvial-fan well logs were previously described by Turk (1973) and Stephens (1974). However, many logs were not reported in these documents and several replacement wells have been drilled and logged since these reports were published. We examined the Utah Division of Water Rights database (2022) to identify additional well logs. We also summarized two ~40-m-deep highway construction sediment logs in the alluvial-fan aquifer area (RS6310 Core1 and Core2) (Utah Department of Transportation, 1969a) (figure 9, table 2). The first significant gravel layer that is most likely to be laterally continu-

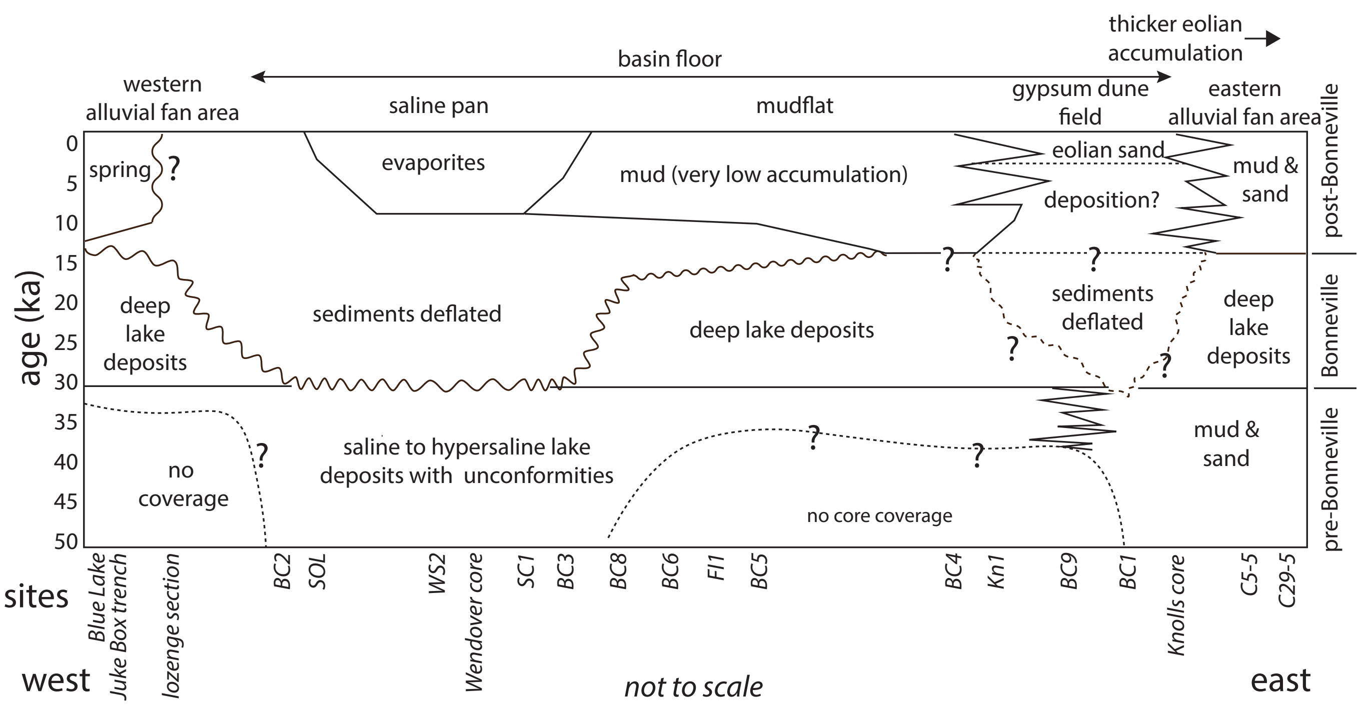


***Figure 8.*** *Chronostratigraphic diagram based on interpreted sediment ages in cores shown in figure 7 (sediment log data sources and location data are summarized in table 1).*

ous occurs at an elevation between 1290 and 1210 m above mean sea level (figure 10). To aid our aquifer interpolation, we also mapped the mountain-front bedrock to alluvial-fan gravel interface at several points. Our model is highly simplified but demonstrates a potential distribution of the uppermost part of the alluvial-fan aquifer.

## Depositional Trends

The spatial distribution of the alluvial-fan aquifer is shown in figures 10 and 11. Thick (>5 m) gravel beds used for brackish water production have high lateral continuity (figure 11) and gravel beds tend to occur at greater depths in the area to the northeast and shallower depths in the areas to the southwest (figure 10). A potential contributor to this spatial pattern is the up-slope alluvial-fan area to the west of these sites. The area between BW-2 and BW-10 has a much larger up-slope alluvial-fan area than the area between BW-16 and BW-20.

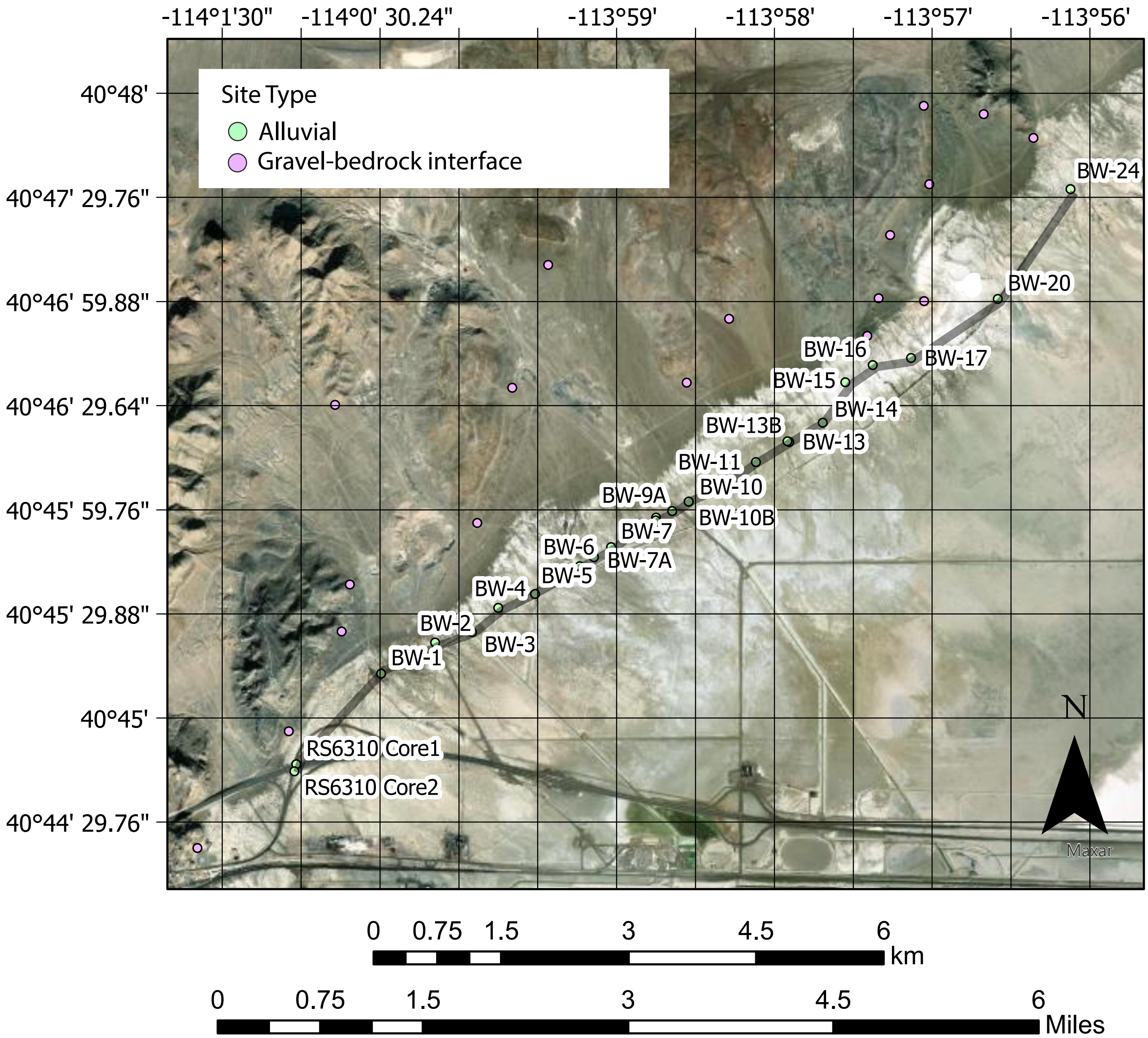


*Figure 9. Location and IDs of well sites and locations of gravel-bedrock interface sites. Southwest-to-northeast cross section line (gray) shown (cross section shown on figure 11).*

***Table 2.*** *Alluvial-Fan Data. Summary of alluvial-fan sediment log data. Note that the accuracy of location was limited in some reports and is noted with an "x" in the "location is approximate" column.*

| Site ID | Total Depth (m) | Latitude DD WGS84 | Longitude DD WGS84 | Location is approximate | Surface Elevation (m asl) | Construction Date | Depth to shallowest gravel (m) | Elevation of shallowest gravel (m asl) | Site Type | Data Source |
|---|---|---|---|---|---|---|---|---|---|---|
| AF-1 | | 40.7964 | -113.9393 | | 1300.89 | | | 1300.8 | gravel-bedrock interface | |
| AF-10 | | 40.7768 | -113.9759 | | 1313.69 | | | 1313.6 | gravel-bedrock interface | |
| AF-11 | | 40.7863 | -113.9906 | | 1399.64 | | | 1399.6 | gravel-bedrock interface | |
| AF-12 | | 40.7764 | -113.9944 | | 1365.50 | | | 1365.5 | gravel-bedrock interface | |
| AF-13 | | 40.7656 | -113.9981 | | 1313.08 | | | 1313.0 | gravel-bedrock interface | |
| AF-14 | | 40.7751 | -114.0131 | | 1421.89 | | | 1421.8 | gravel-bedrock interface | |
| AF-15 | | 40.7607 | -114.0115 | | 1333.80 | | | 1333.8 | gravel-bedrock interface | |
| AF-16 | | 40.7569 | -114.0124 | | 1316.13 | | | 1316.1 | gravel-bedrock interface | |
| AF-17 | | 40.7489 | -114.0180 | | 1306.37 | | | 1306.3 | gravel-bedrock interface | |
| AF-18 | | 40.7396 | -114.0276 | | 1304.54 | | | 1304.5 | gravel-bedrock interface | |
| AF-2 | | 40.7983 | -113.9446 | | 1339.60 | | | 1339.5 | gravel-bedrock interface | |
| AF-3 | | 40.7990 | -113.9509 | | 1367.03 | | | 1367.0 | gravel-bedrock interface | |
| AF-4 | | 40.7927 | -113.9503 | | 1320.09 | | | 1320.0 | gravel-bedrock interface | |
| AF-5 | | 40.7887 | -113.9544 | | 1318.87 | | | 1318.8 | gravel-bedrock interface | |
| AF-6 | | 40.7834 | -113.9508 | | 1297.23 | | | 1297.2 | gravel-bedrock interface | |
| AF-7 | | 40.7836 | -113.9557 | | 1321.31 | | | 1321.3 | gravel-bedrock interface | |
| AF-8 | | 40.7806 | -113.9569 | | 1299.97 | | | 1299.9 | gravel-bedrock interface | |
| AF-9 | | 40.7820 | -113.9715 | | 1339.60 | | | 1339.5 | gravel-bedrock interface | |
| BW-1 | 32.0 | 40.7536 | -114.0082 | | 1289.91 | 1946 | 19.2 | 1273.7 | alluvial | Utah Water Rights website |
| BW-10 | 66.8 | 40.7673 | -113.9757 | | 1288.32 | 1947 | 16.2 | 1271.8 | alluvial | Utah Water Rights website |
| BW-10B | 67.1 | 40.7673 | -113.9757 | | 1288.32 | 1997 | | | alluvial | Utah Water Rights website |
| BW-11 | 75.3 | 40.7690 | -113.9721 | | 1287.77 | 1948 | 46 | 1243.9 | alluvial | Utah Water Rights website |
| BW-12 | 85.3 | 40.7705 | -113.9686 | | 1287.94 | 1948 | 46 | 1244.2 | alluvial | Utah Water Rights website |
| BW-13 | 68.6 | 40.7721 | -113.9651 | | 1288.40 | 1947 | 42 | 1247.6 | alluvial | Utah Water Rights website |
| BW-13B | 92.1 | 40.7722 | -113.9653 | | 1288.40 | 2001 | | | alluvial | Utah Water Rights website |
| BW-14 | 75.3 | 40.7736 | -113.9616 | | 1288.72 | 1948 | 47.2 | 1242.7 | alluvial | Utah Water Rights website |
| BW-15 | 50.0 | 40.7769 | -113.9592 | | 1289.77 | 1948 | 30.5 | 1260.9 | alluvial | Utah Water Rights website |
| BW-16 | 87.5 | 40.7782 | -113.9563 | | 1289.00 | 1948 | 76 | 1213.3 | alluvial | Utah Water Rights website |
| BW-17 | 110.9 | 40.7788 | -113.9522 | | 1289.91 | 1948 | 73.8 | 1216.1 | alluvial | Utah Water Rights website |
| BW-2 | 48.8 | 40.7560 | -114.0025 | | 1289.91 | 1946 | 16 | 1275.8 | alluvial | Utah Water Rights website |
| BW-20 | 89.9 | 40.7835 | -113.9431 | | 1289.30 | 1947 | 75.3 | 1214.0 | alluvial | Utah Water Rights website |
| BW-24 | 50.9 | 40.7923 | -113.9354 | | 1289.24 | 1948 | 42.7 | 1247.7 | alluvial | Utah Water Rights website |
| BW-3 | 53.6 | 40.7569 | -113.9986 | | 1289.30 | 1948 | 16 | 1274.3 | alluvial | Utah Water Rights website |
| BW-4 | 53.6 | 40.7588 | -113.9958 | | 1289.30 | 1948 | 18 | 1273.4 | alluvial | Utah Water Rights website |
| BW-5 | 65.8 | 40.7599 | -113.9920 | | 1289.30 | 1948 | 28.42 | 1263.3 | alluvial | Utah Water Rights website |
| BW-6 | 53.0 | 40.7622 | -113.9872 | | 1288.60 | 1948 | 35.1 | 1256.3 | alluvial | Utah Water Rights website |
| BW-7 | 53.3 | 40.7637 | -113.9839 | | 1288.56 | 1948 | 41.8 | 1249.6 | alluvial | Utah Water Rights website |
| BW-7A | 53.2 | 40.7629 | -113.9857 | | 1288.04 | 1949 | 41.8 | 1245.6 | alluvial | Utah Water Rights website |
| BW-8 | 56.4 | 40.7645 | -113.9825 | | 1288.95 | 1946 | 43 | 1248.4 | alluvial | Utah Water Rights website |
| BW-8A | 64.0 | 40.7649 | -113.9806 | | 1288.95 | 1949 | | | alluvial | Utah Water Rights website |
| BW-8B | 74.2 | 40.7646 | -113.9820 | | 1288.95 | 2021 | | | alluvial | Utah Water Rights website |
| BW-9 | 55.2 | 40.7660 | -113.9792 | | 1288.08 | 1947 | 43.5 | 1244.5 | alluvial | Utah Water Rights website |
| BW-9A | 58.8 | 40.7666 | -113.9775 | | 1288.08 | 1949 | | | alluvial | Utah Water Rights website |
| BW-9B | 67.1 | 40.7658 | -113.9792 | | 1289.06 | 1995 | | | alluvial | Utah Water Rights website |
| RS6310 Core1 | 37.0 | 40.7463 | -114.0172 | x | 1294.18 | 1968 | 9.5 | 1284.6 | alluvial | Highway construction boring log; Utah Department of Transportation, 1969a |
| RS6310 Core2 | 42.0 | 40.7457 | -114.0174 | x | 1294.18 | 1968 | 9.3 | 1284.8 | alluvial | Highway construction boring log; Utah Department of Transportation, 1969a |

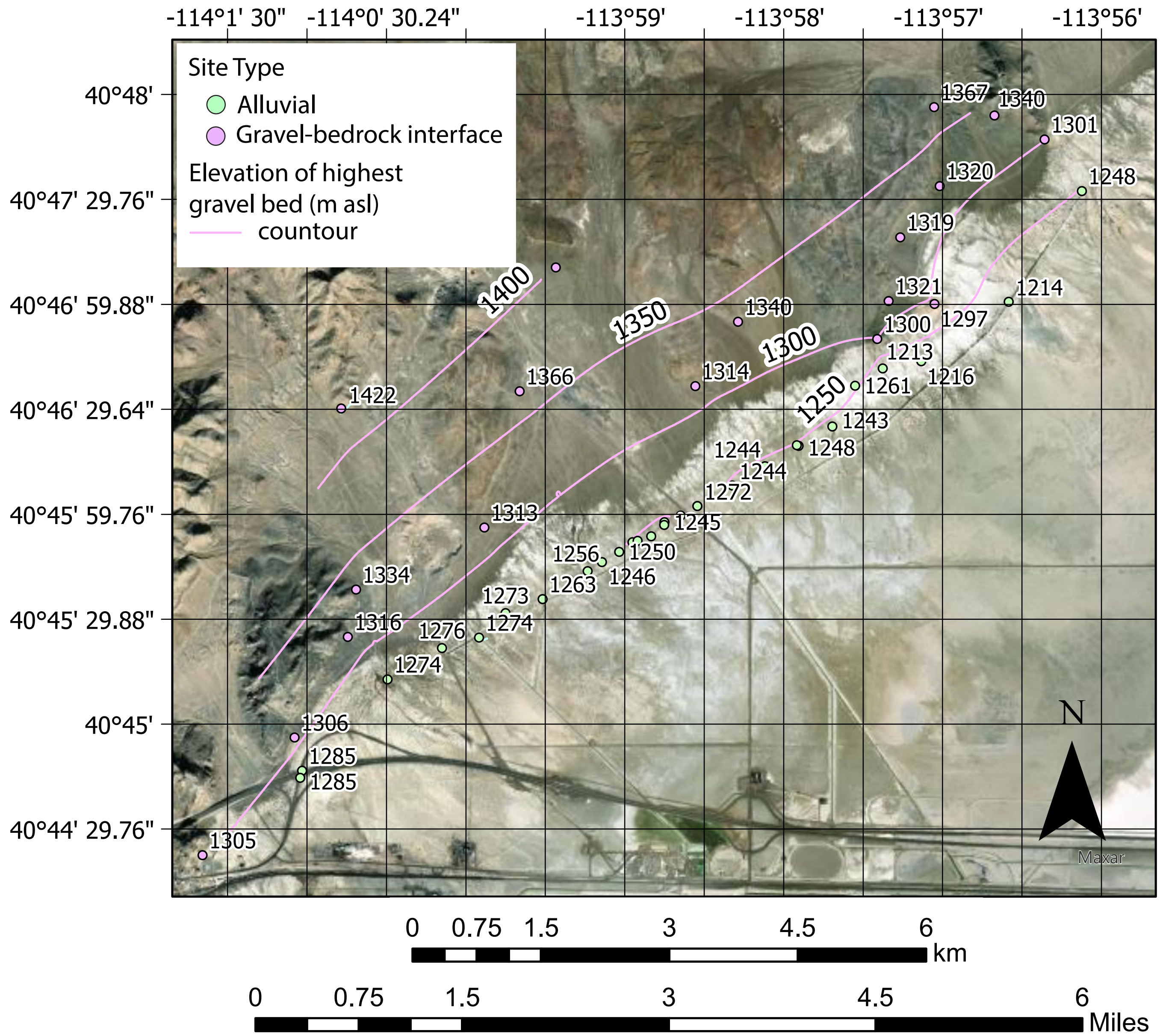


***Figure 10.*** *Elevation (m above mean sea level) of highest gravel layer in alluvial-fan sites (50 m contour interval). See figure 9 for location IDs.*

## Deep Wells

Deep GSLD wells have been drilled for highway construction evaluation, oil and gas and mineral exploration, and scientific purposes (figure 12, table 3). One highway construction assessment sediment log was collected in the area to the southwest of the Bonneville Salt Flats (RS6311) (Utah Department of Transportation, 1969b). Where data was sufficient, we noted the elevation of the highest significant gypsum layer (figure 13) and the highest significant gravel layer (figure 14). We also created east-to-west (figure 15) and north-to-south-to-east cross sections (figure 16) of deep wells.

### Oil and Gas Exploration Wells

Two exploratory oil and gas wells were drilled in the Bonneville Salt Flats area. The Shell Salduro No. 1 (43-045-11076) well was drilled in 1956 and the Alpha Minerals, Inc. (C-1-17)34ba-1 (43-045-30001) well was drilled in 1975 (Utah Division of Oil, Gas and Mining, 2023). Aspects of these wells are described and analyzed in several publications (Whelan and Petersen, 1974; Lines, 1979; Smith and others, 2012).

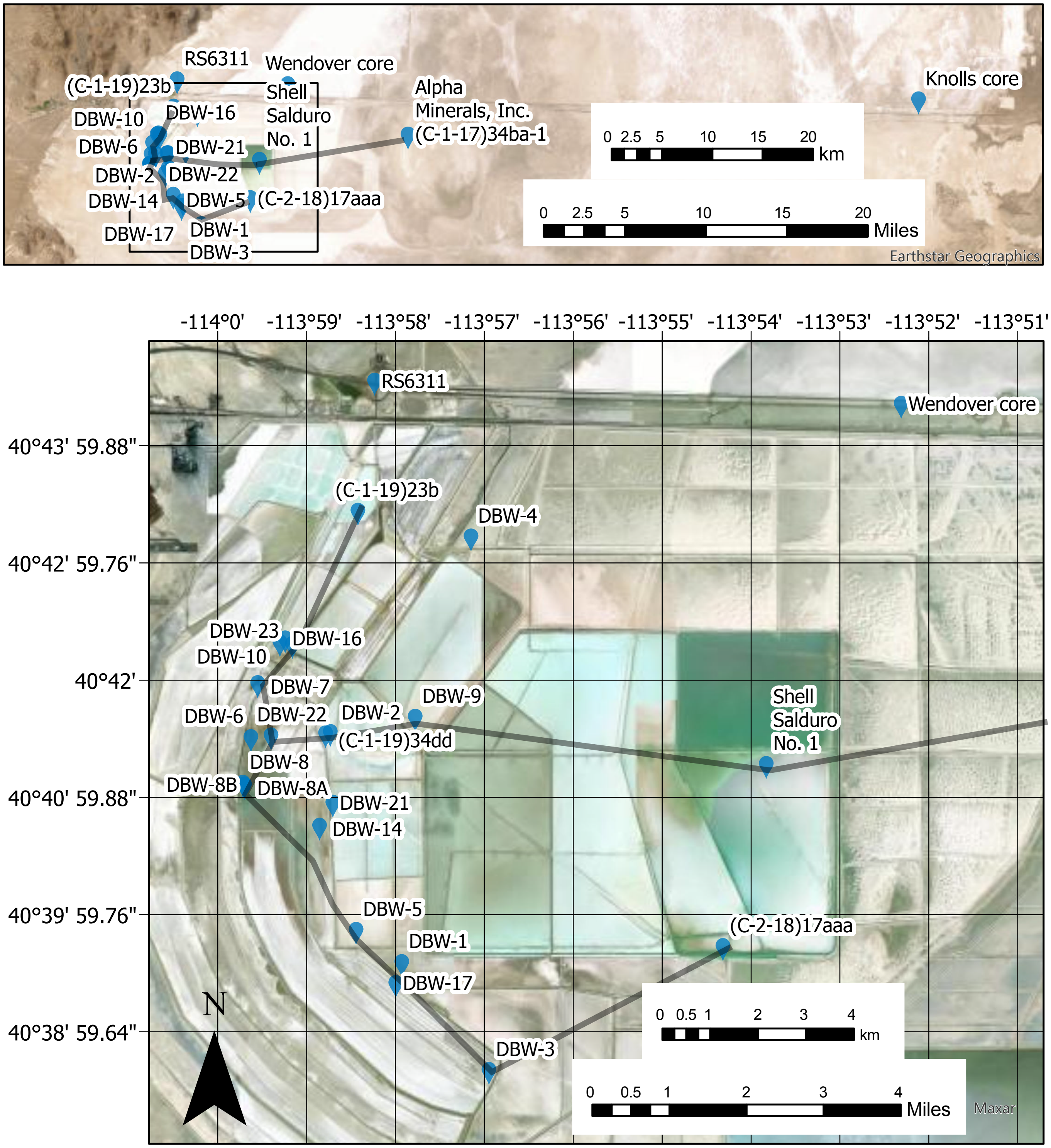


***Figure 12.*** *Location and IDs of deep wells with logs. Note locations of west-to-east and north-to-south-to-east cross sections (gray lines) (cross sections shown on figures 15 and 16, respectively).*

***Table 3:*** *Deep Well Data. Summary of deep well sediment log data. Note that the accuracy of location was limited in some reports and is noted with an "x" in the "location is approximate" column.*

| SiteID | Total Depth (m) | Latitude DD WGS84 | Longitude DD WGS84 | Location is approximate | Surface Elevation (m asl) | Construction Date | Depth to highest gypsum (m) | Highest gypsum elevation (m asl) | Depth to highest gravel (m) | Highest gravel elevation (m asl) | Data Source |
|---|---|---|---|---|---|---|---|---|---|---|---|
| DBW-2 | 469 | 40.6905 | -113.9789 | x | 1286.26 | 1949 | 82 | 1204.26 | 309 | 977 | Turk, 1973 |
| DBW-3 | 630 | 40.6424 | -113.9491 | x | 1284.76 | 1950 | 76 | 1208.76 | 371 | 914 | Turk, 1973 |
| DBW-5 | 469 | 40.6623 | -113.9741 | x | 1284.83 | 1950 | 86 | 1198.83 | 340 | 945 | Turk, 1973 |
| DBW-6 | 352 | 40.6898 | -113.9938 | x | 1284.73 | 1950 | 80.77 | 1203.96 | 287.7 | 997 | Turk, 1973 |
| DBW-8 | 343 | 40.6833 | -113.9953 | x | 1285.04 | 1950 | 81.7 | 1203.34 | 283.4 | 1002 | Turk, 1973 |
| DBW-7 | 326 | 40.6974 | -113.9925 | x | 1284.53 | 1950 | 140.5 | 1144.03 | 280 | 1005 | Utah Water Rights website |
| DBW-4 | 500 | 40.7183 | -113.9525 | x | 1286.26 | 1951 | 65.8 | 1220.46 | 374.9 | 911 | Turk, 1973 |
| DBW-1 | 366 | 40.6578 | -113.9655 | x | 1285.04 | 1951 | 82.3 | 1202.74 | 356 | 929 | Turk, 1973 |
| DBW-9 | 432 | 40.6926 | -113.9630 | x | 1284.29 | 1951 | | | 310.89 | 973 | Utah Water Rights website |
| DBW-10 | 351 | 40.7033 | -113.9883 | x | 1286.26 | 1951 | 82 | 1204.26 | 309.7 | 977 | Turk, 1973 |
| Shell Salduro No. 1 | 899 | 40.6859 | -113.8972 | x | 1284.86 | 1956 | 103.63 | 1181.23 | 411.5 | 873 | Utah Mineral Rights website: https://dataexplorer.ogm.utah.gov/; Whelan and Petersen 1974 |
| Knolls core | 152 | 40.7269 | -113.3090 | x | 1291.00 | 1960 | | | | | Williams, 1994; Shuey, 1971 |
| Wendover core | 171 | 40.7371 | -113.8719 | x | 1285.00 | 1960 | 76-91 | | | | Williams, 1994; Shuey, 1971 |
| RS6311 | 32 | 40.7404 | -113.9706 | x | 1288.08 | 1968 | | | | | Highway construction boring log; Utah Department of Transportation, 1969b |
| Alpha Minerals, Inc. (C-1-17)34ba-1 | 1298 | 40.7030 | -113.7645 | | 1286.87 | 1975 | 45.7 | 1241.17 | 137 | 1150 | Lines, 1979 (log by T.R. Blazzard); https://dataexplorer.ogm.utah.gov/ |
| DBW-14 | 463 | 40.6772 | -113.9809 | x | 1284.77 | 1978 | | | 320 | 965 | Utah Water Rights website |
| (C-1-19)23b | 460 | 40.7219 | -113.9737 | x | 1285.65 | 1979 | 97.5 | 1188.15 | 301.75 | 984 | Utah Water Rights website |
| DBW-16 | 462 | 40.7038 | -113.9873 | x | 1285.74 | 1989 | | | 295.65 | 990 | Utah Water Rights website |
| DBW-17 | 458 | 40.6548 | -113.9666 | x | 1284.77 | 1990 | | | 344.4 | 940 | Utah Water Rights website |
| DBW-8A | 458 | 40.6830 | -113.9950 | x | 1284.08 | 1990 | 140 | 1144.08 | 256 | | Utah Water Rights website |
| DBW-21 | 413 | 40.6804 | -113.9784 | x | 1284.77 | 2004 | | | 317 | 968 | Utah Water Rights website |
| DBW-8B | 413 | 40.6830 | -113.9950 | x | 1284.08 | 2006 | 109.7 | 1174.38 | 316.99 | | Utah Water Rights website |
| DBW-23 | 485 | 40.7030 | -113.9860 | x | 1284.92 | 2008 | | | 281.9 | | Utah Water Rights website |
| DBW-22 | 481 | 40.6900 | -113.9900 | x | 1284.16 | 2008 | | | 278.9 | 1005 | Utah Water Rights website |
| (C-1-19)34dd | 479 | 40.6903 | -113.9798 | | 1283.93 | 2013 | 70.1 | 1213.83 | 448 | | Utah Water Rights website |
| (C-2-18)17aaa | 470 | 40.6600 | -113.9053 | | 1284.77 | 2013 | 158.5 | 1126.27 | 345 | 940 | Utah Water Rights website |

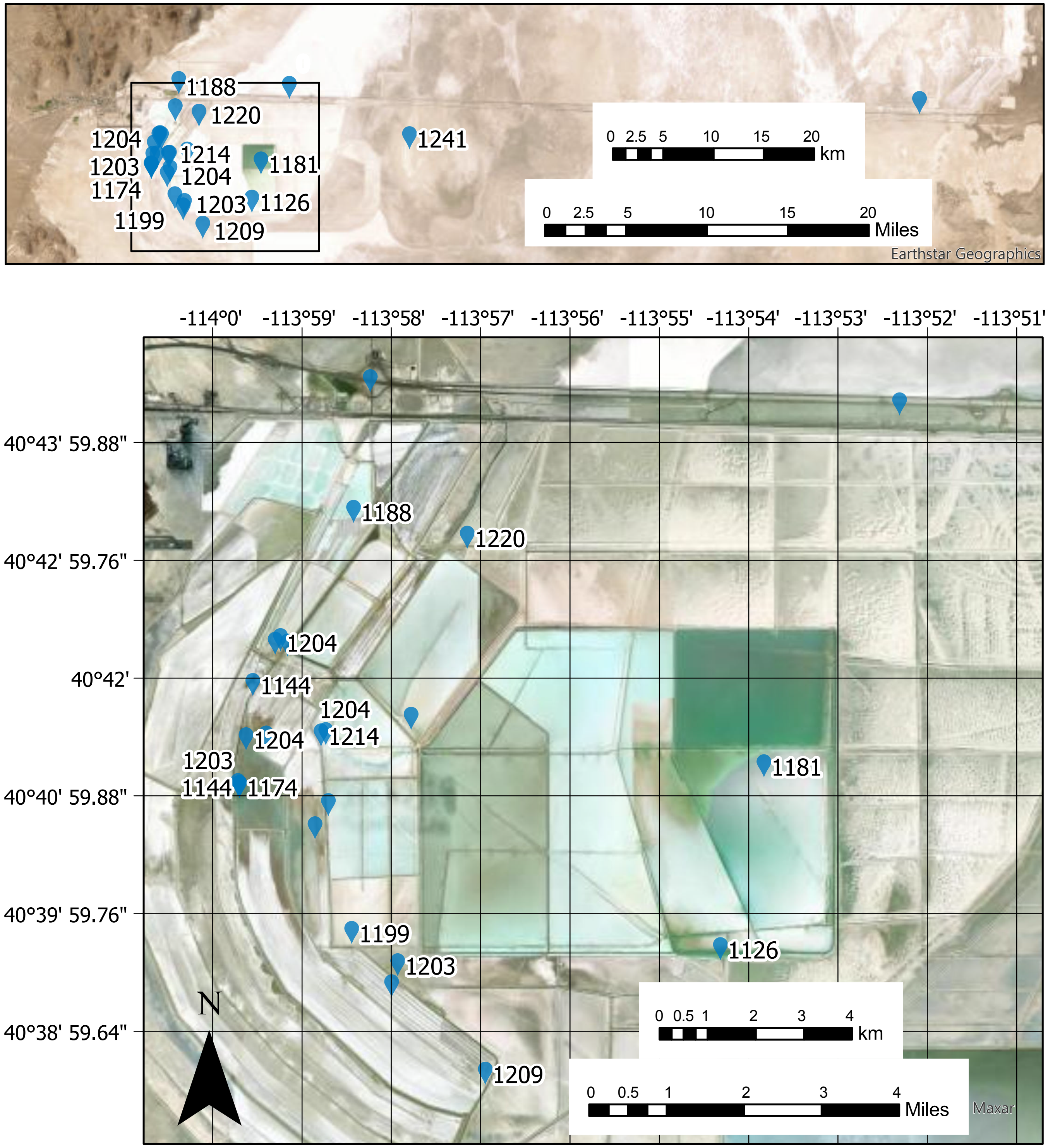


***Figure 13.*** *Elevation (m above sea level) of highest significant gypsum layer in deep well sites.*

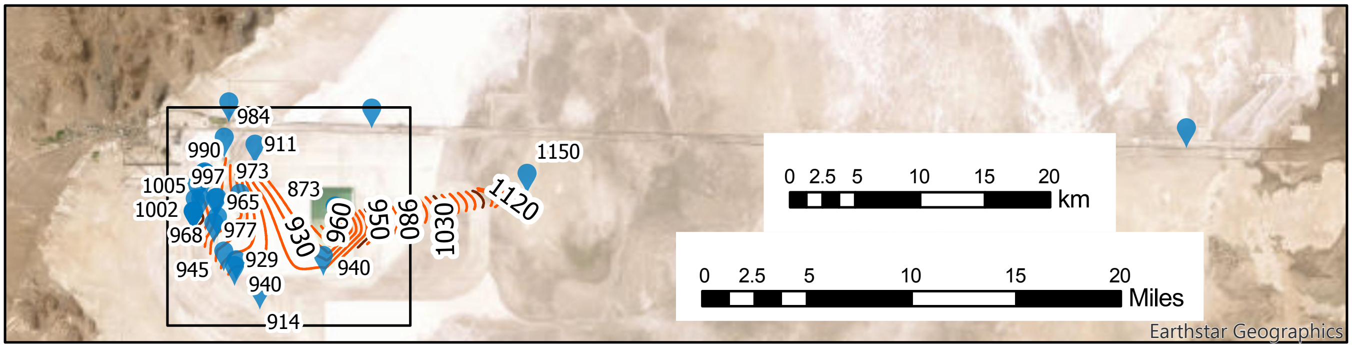


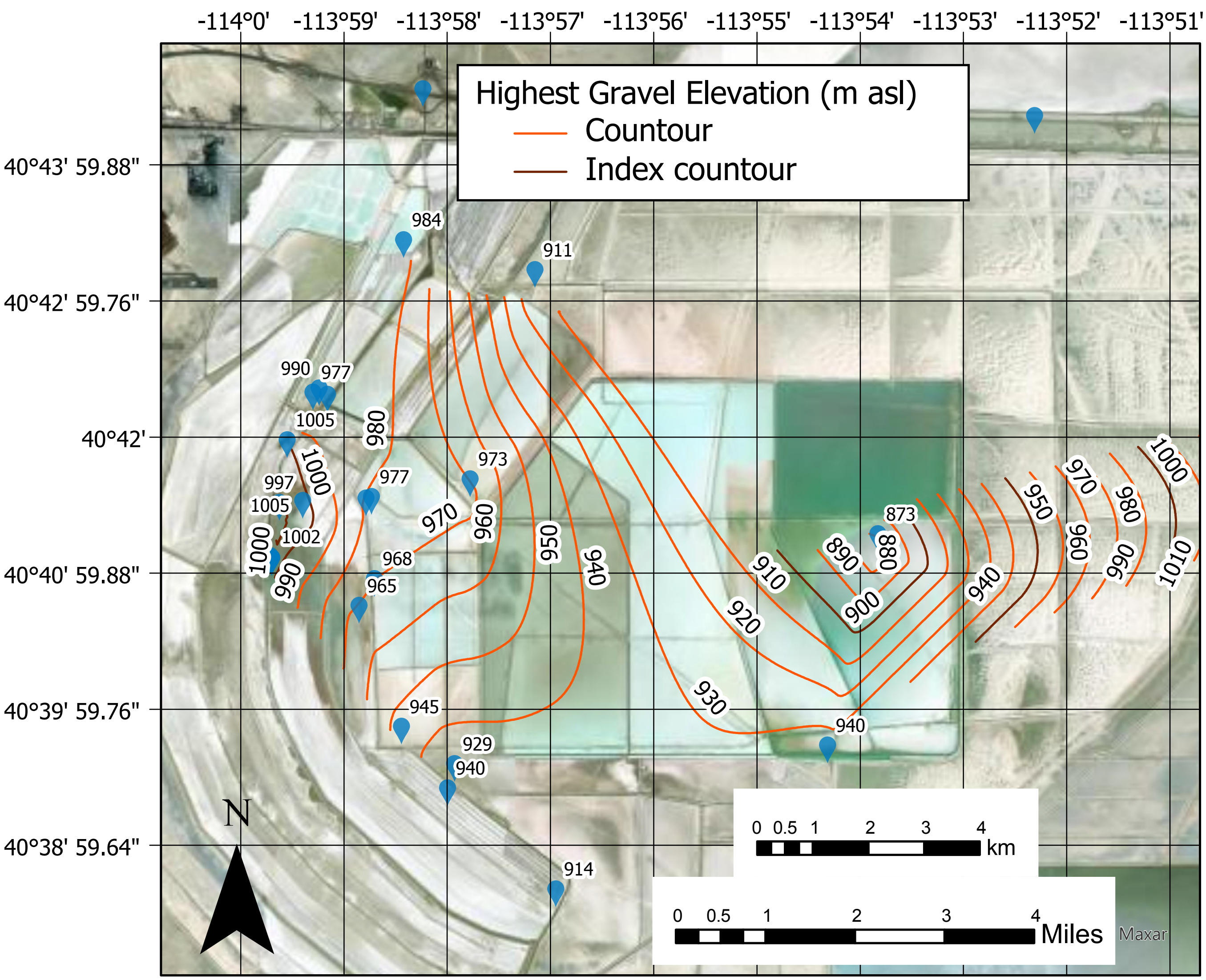


*Figure 14. Elevation (m above mean sea level) of the highest significant gravel layer in deep well sites and contours (10 m contour interval) interpolated from that data. Higher contour uncertainty areas in the center and to the east.*

### Scientific Cores

The Knolls and Wendover cores were drilled for scientific research by the University of Utah in 1960. Aspects of these cores are described in Martin and Mehringer (1965), Shuey (1971), Williams (1994), and Bright and others (2022). Magnetostratigraphy, palynology, tephrochronology, amino-acid racemization, and radiocarbon dating of sediments were used to construct age-depth curves (figure 17, table 4).

### Deep Brine Wells

We documented more than 20 deep brine wells at the site of the potash mine but sediment logs were not available for every well. Some of these wells are described in Turk (1973), Stephens (1974), Whelan and Petersen (1974), and Smith and others (2012). We examined the Utah Division of Water Rights database to identify logs from additional wells that were not described in those publications. Most of these wells are several decades old and are no longer active.

### Depositional Trends

There is large variation in the depth of the highest significant gypsum and gravel interval across adjacent wells because of differences in logging interpretations (figures 15 and 16). In aggregate, these data show larger trends. Many gypsum beds underlie the uppermost gypsum layer, as noted in our study, but no non-Holocene gypsum beds are logged between the uppermost gypsum bed and the surface. The first gypsum interval appears to occur at a greater depth at the center of the Wendover graben. If this interval was deposited as a continuous horizontal layer, then the center of the Wendover graben has subsided since the gypsum layer was deposited. Based on an estimated depth between 71 and 91 m for the first large gypsum layer in the Wendover Core, and using the Wendover Core's age-depth model (figure 17), we estimate preservation/deposition of gypsum in this area ceased at approximately 600–750 ka. This timing corresponds to the period immediately prior to the Lava Creek lake at ~620 ka (Oviatt and others, 1999). Paleosol deposition was noted in the Knolls Core prior to this time, in contrast to the gypsum observed in the Salduro core (Shuey, 1971). The uppermost gravel interval was more consistently logged across cores than gypsum was and shows approximately 250 m of vertical offset between the center of the Wendover graben and the area outside of the graben to the east (figure 15).

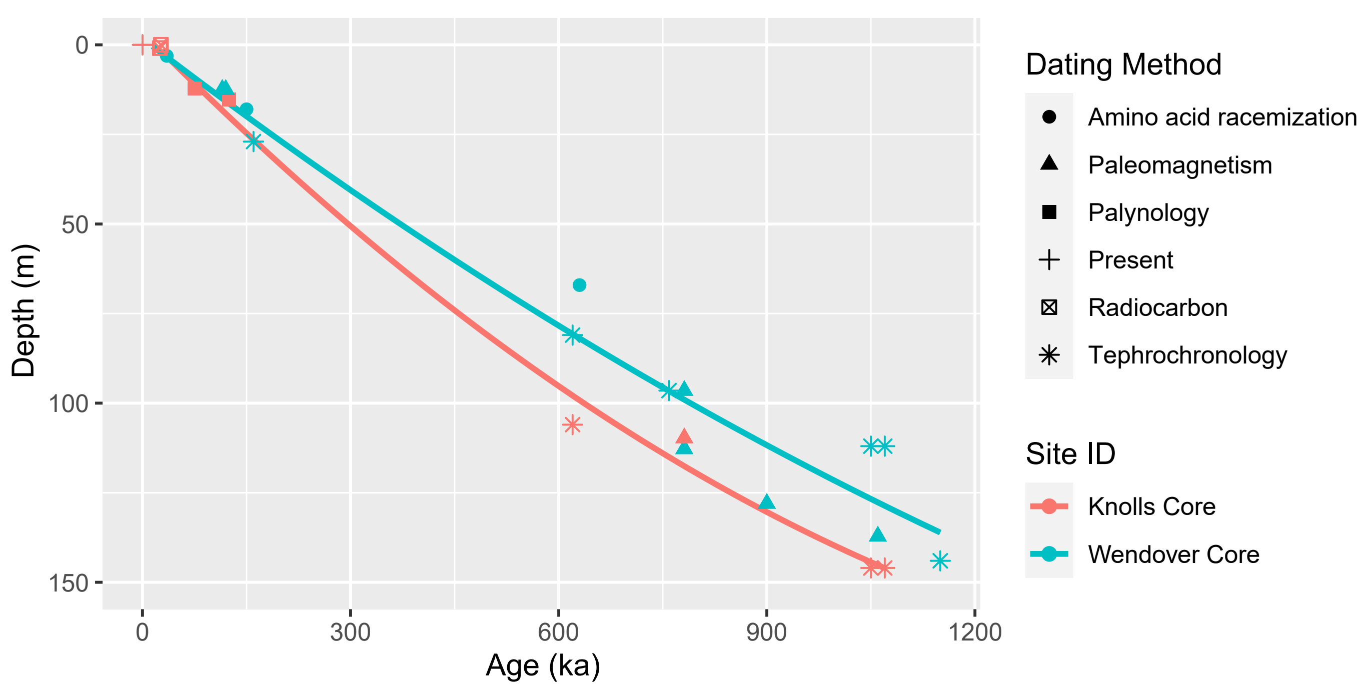


*__Figure 17.__ Age-depth model for Wendover and Knolls cores. Model is based on information from Eardley (1962), Martin and Mehringer (1965), Shuey (1971), Williams (1994), and Bright and others (2022); these data are summarized in table 4.*

***Table 4:*** *Wendover Core and Knolls Core Age-Depth Data. Chronological constraints on the depositional record of the Wendover and Knolls cores.*

| Site ID | Depth (m) | Age (ka) | Description | Dating Method | Data Source |
|---|---|---|---|---|---|
| Knolls Core | 0.0 | 0 | top of core, present | present | |
| Knolls Core | 0.0 | 26.5 | bulk sed. radiocarbon 26.5±2 cal ka at surface, 25.1±1.6 cal kyr B.P. at ~1 m depth | radiocarbon | Eardley, 1962 |
| Knolls Core | 0.9 | 25.1 | bulk sed. radiocarbon 26.5±2 cal ka at surface, 25.1±1.6 cal kyr B.P. at ~1 m depth | radiocarbon | Eardley, 1962 |
| Knolls Core | 12.2 | 75 | pollen free zone (interpreted as Sangamon interglacial: 75-125 ka) | palynology | Shuey, 1971; Martin and Mehringer, 1965 |
| Knolls Core | 15.2 | 125 | pollen free zone (interpreted as Sangamon interglacial: 75-125 ka) | palynology | Shuey, 1971; Martin and Mehringer, 1965 |
| Knolls Core | 106.0 | 620 | Lava Creek B ash (0.62 Ma) | tephrastratigraphy | Williams, 1994 |
| Knolls Core | 109.7 | 781 | suspect Brunhes/Matuyama boundary at or above this (~0.781 Ma) | paleomagnetism | Shuey, 1971 |
| Knolls Core | 146.0 | 1050 | Glass Mountain D ash (?) (1.06 ± 0.01 Ma) | tephrastratigraphy | Williams, 1994 |
| Knolls Core | 146.0 | 1070 | Glass Mountain D ash (?) (1.06 ± 0.01 Ma) | tephrastratigraphy | Williams, 1994 |
| Wendover Core | 0.0 | 0 | top of core, present | present | |
| Wendover Core | 3.1 | 35 | amino acid racemization, slightly older than Lake Bonneville (~35 ka) | amino acid racemization | Bright and others, 2022 |
| Wendover Core | 12.2 | 75 | pollen free zone (interpreted as Sangamon interglacial: 75-125 ka) | palynology | Shuey, 1971; Martin and Mehringer, 1965 |
| Wendover Core | 12.5 | 115 | suspect Blake event (0.115-0.120 Ma) | paleomagnetism | Shuey, 1971 |
| Wendover Core | 12.5 | 120 | suspect Blake event (0.115-0.120 Ma) | paleomagnetism | Shuey, 1971 |
| Wendover Core | 15.2 | 125 | pollen free zone (interpreted as Sangamon interglacial: 75-125 ka) | palynology | Shuey, 1971; Martin and Mehringer, 1965 |
| Wendover Core | 18.0 | 150 | amino acid racemization (Bright and others, 2022), Little Valley Lake equivalent (~150 ka) | amino acid racemization | Bright and others, 2022 |
| Wendover Core | 27.0 | 160 | Pahoa Island ash (~0.16 Ma) | tephrastratigraphy | Williams, 1994 |
| Wendover Core | 67.1 | 630 | amino acid racemization, Little Creek Lake equivalent (~630 ka) | amino acid racemization | Bright and others, 2022 |
| Wendover Core | 81.0 | 620 | Lava Creek B ash (0.62 Ma) | tephrastratigraphy | Williams, 1994 |
| Wendover Core | 96.5 | 759 | Bishop ash (0.759 Ma) | tephrastratigraphy | Williams, 1994 |
| Wendover Core | 96.5 | 781 | suspect Brunhes/Matuyama boundary (~0.781 Ma) | paleomagnetism | Shuey, 1971 |
| Wendover Core | 112.0 | 1050 | Glass Mountain D ash (?) (1.06 ± 0.01 Ma) | tephrastratigraphy | Williams, 1994 |
| Wendover Core | 112.0 | 1070 | Glass Mountain D ash (?) (1.06 ± 0.01 Ma) | tephrastratigraphy | Williams, 1994 |
| Wendover Core | 112.8 | 781 | suspect Brunhes/Matuyama boundary (~0.781 Ma) | paleomagnetism | Shuey, 1971 |
| Wendover Core | 128.0 | 900 | suspect Jarmillo event (lower confidence) (~0.9-1.06 Ma) | paleomagnetism | Shuey, 1971 |
| Wendover Core | 137.2 | 1060 | suspect Jarmillo event (lower confidence) (~0.9-1.06 Ma) | paleomagnetism | Shuey, 1971 |
| Wendover Core | 144.0 | 1150 | Bailey ash (1.15 Ma) | tephrastratigraphy | Williams, 1994 |

# DISCUSSION

## Distribution of Deflation

The thickest Holocene and Lake Bonneville deposits occur at the edges of GSLD, distal to the basin floor. Deflation has removed all Lake Bonneville sediments in the areas surrounding the Bonneville Salt Flats, whereas Bonneville sediments are partially deflated (and may be absent in some areas) near the Knolls sand dunes area. Surprisingly, because of the deflation of Lake Bonneville sediments, the Bonneville Salt Flats, a Holocene GSLD depositional area with up to ~1.5 m of deposition, has a more incomplete geologic record than the adjoining mudflat, which has had little, if any Holocene deposition but has retained some to all of Lake Bonneville marl deposits. The Bonneville Salt Flats is a modern GSLD regional low, and waters from across GSLD are concentrated here, with their solutes contributing to the saline pan. If the Bonneville Salt Flats site was a regional low in the past, as its location in the Wendover graben suggests, then it is likely that the stratigraphic record here will have more deflationary periods with greater amounts of deflation than slightly higher basin floor areas. This highlights the potential for regional lows in arid climates to have more incomplete geologic records, making this an important consideration when planning and interpreting investigations of paleoenvironmental records. We anticipate possible erosion and absence of sediments from large pre-Lake Bonneville Quaternary lakes at this site relative to other locations (for example, the cores described in Williams, 1994; and in Oviatt and others, 1999).

### Deflationary Model

Research on similar saline pans and playas indicates that these landforms are highly sensitive to groundwater levels and are most likely to become deflationary surfaces, where sediment is removed by wind, when groundwater levels are below the surface (Rosen, 1994). Although this may explain deflation of Lake Bonneville sediments at the Bonneville Salt Flats, it does not explain why the Bonneville Salt Flats area would be more eroded than higher areas to the east, as we would anticipate groundwater levels to be lower in those areas. Depositional and deflationary models from White Sands National Park, New Mexico, suggest that freshwater lenses hosted in dune fields, and associated vegetation maintained by this fresh water, may limit deflation in higher areas relative to lower-lying, more saline, areas (Langford, 2003; Langford and others, 2009).

Although prior models may partially explain observed deflationary patterns at the Bonneville Salt Flats, research on modern deflation at Owens Lake, California, provides a model that may best explain observed patterns (figure 18) (Reynolds and others, 2007). In addition to groundwater level, Reynolds and others (2007) considered the impact of groundwater salinity and evaporite growth on surface stability. They observed that mudflats with less saline groundwaters can form very stable surfaces that are somewhat resistant to erosion. As the groundwater salinity increases and groundwater evaporation rises, efflorescent salt crusts and displacive minerals develop. Efflorescent crusts easily break when disturbed or windblown; after breaking they are transported across the surface, acting as a surface abrasive that enables the generation of easily deflated dust-sized particles. Displacive minerals, similarly, disrupt subsurface sediments, altering their texture, possibly making them more susceptible to deflation. Only when groundwater salinity has risen high enough to support a saline crust and groundwater levels are high can a stable saline crust (in this case, halite) form. In particular, crusts crystalized from surface waters can form the thickest and most stable crusts, which are highly resistant to erosion (figure 18B).

Based on our model, we can predict how the Bonneville Salt Flats landscape may have evolved between Lake Bonneville and the later deposition of a stable halite crust. Following Lake Bonneville, this area was likely a somewhat stable mudflat. As a regional low, solutes concentrated in this area increased groundwater salinity over time. Also, as the salinity rose, efflorescent surface crystals and displacive crystals formed, enabling elevated deflation to occur. Eventually, this system reached a tipping point where groundwater salinity was high enough to sustain a saline crust. Once a sustained saline crust developed, deflation ceased at the saline pan, but may have continued at its edges, which may partially explain why pre-Lake Bonneville strata are thickest at the center of the modern saline pan and then thin to its edges (Bernau and others, in review).

### Potential Impact of Deflation on Shallow Brine Aquifer

The shallow brine aquifer occurs in shallow basinal muds from 0 to <10 m depth (Turk and others, 1973) and is the primary source of brine for potash production. Christiansen and Patil (1962) reported a sharp decrease in shallow brine aquifer permeability at mile marker 17 (approximately 40.7323° N, 113.7174° W, WGS84 datum) and beyond to the east towards Knolls (along I-80) relative to areas closer to the salt flats (Christiansen and others, 1960a, 1960b). The decrease in permeability is associated with the presence of Lake Bonneville sediments; correspondingly, deflation is associated with increased permeability in the shallow brine aquifer. Turk and others (1973) described the shallow brine aquifers' high hydraulic conductivity and partially attributed this property to fractures in the sediment, which may be associated with desiccation.

## CONCLUSIONS

We have compiled and interpreted sediment logs across the Great Salt Lake Desert, with a focus on the Bonneville Salt Flats area. These data provide context for understanding geological structures and aquifers in this region, and show that basin floor deposition and erosion is laterally heterogeneous. Furthermore, they demonstrate a high degree of heterogeneity in sediment preservation in arid regions over time, with modern regional lows sometimes having more incomplete records than adjoining areas. Changes in topography, groundwater levels, and groundwater salinity over time contribute to surface mineralogy, depositional rates, and erosional potential.

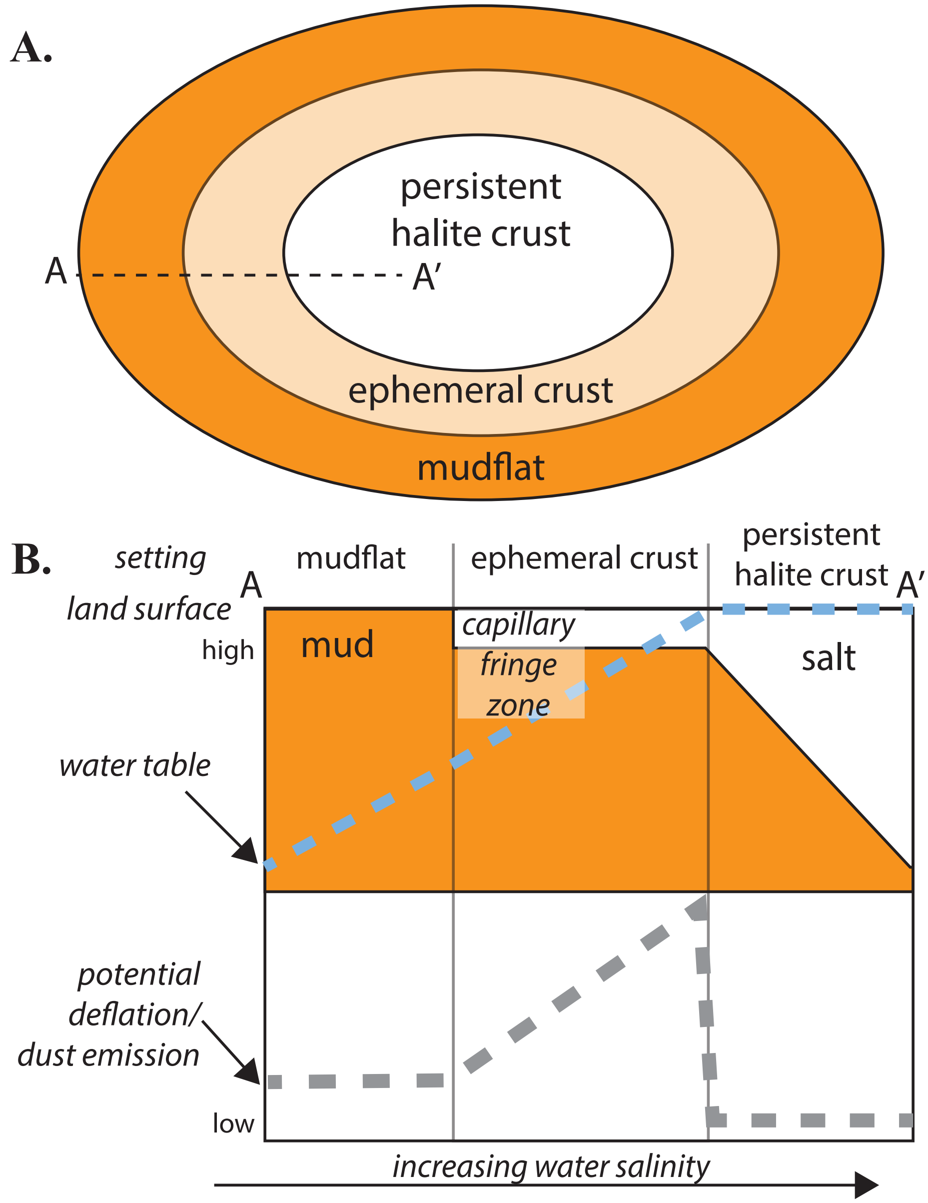


***Figure 18.*** *Deflation model for GSLD (modified from Reynolds and others,2007).* ***(A)*** *Spatial distribution of surface morphology in the saline pan and surrounding area. A - A', the cross section in B, shows deflation is highest in the area immediately adjacent to the persistent saline crust.* ***(B)*** *Model of deflation/deposition in relation to surface morphology and water table level.*

## ACKNOWLEDGMENTS

We acknowledge that this study was conducted on traditionally Newe/Western Shoshone and Goshute lands. We thank Craig Peterson and Russ Draper with Intrepid Potash; the Bureau of Land Management West Desert District's current and former office staff, including Kevin Oliver, Matt Preston, Mike Nelson, Cheryl Johnson, Steve Allen, Roxanne Tea, Michael Gates, Jessica Wade, and Todd Marks; the University of Utah researchers Jory Lerback, Evan Kipnis, Mark Radwin, Benjamin Marconi, Isaac Hart, and Andrea Brunelle; Peter Nielsen and Katie Cummings (former Core Center curators), and Tom Dempster, Utah Core Research Center; and Utah Geological Survey geologists Paul Inkenbrandt, Hugh Hurlow, Greg Gavin, and Elliot Jagniecki. Funding for this work was provided by an NSF Coupled Natural Human Systems Award #1617473, the Utah Geological Survey, the Utah State Legislature, the Bureau of Land Management, an American Association of Petroleum Geologists Grant-In-Aid, and the University of Utah Global Change and Sustainability Center graduate student research grants. Funding for geologic mapping in the area is by the STATEMAP and FEDMAP components of the National Cooperative Geologic Mapping Program.

# REFERENCES


Badri, M., and Mooney, H.M., 1987, Q measurements from compressional seismic waves in unconsolidated sediments: Geophysics, v. 52, no. 6, p. 772–784.

Benson, L. V., Lund, S.P., Smoot, J.P., Rhode, D.E., Spencer, R.J., Verosub, K.L., Louderback, L.A., Johnson, C.A., Rye, R.O., and Negrini, R.M., 2011, The rise and fall of Lake Bonneville between 45 and 10.5 ka: Quaternary International, v. 235, no. 1–2, p. 57–69, https://doi.org/10.1016/j.quaint.2010.12.014.

Bernau, J.A., 2022, Spatial and temporal scales of water and salt movement at the Bonneville Salt Flats: Salt Lake City, University of Utah, Ph.D. dissertation, 195 p.

Bernau, J., Bowen, B., Oviatt, C.G., and Clark, D.L., 2023 (in review), Lateral and temporal constraints on the depositional history of the Bonneville Salt Flats, USA: Quaternary Research.

Bingham, C.P., 1980, Solar production of potash from the brines of the Bonneville Salt Flats, *in* Gwynn, J.W., editor, Great Salt Lake—a scientific, historical and economic overview: Utah Geological and Mineral Survey Bulletin 116, p. 229–242, https://doi.org/10.34191/b-116.

Bissell, H.J., and Chilingar, G. V., 1962, Evaporite type dolomite in Salt Flats of western Utah: Sedimentology, v. 1, no. 3, p. 200–210, https://doi.org/10.1111/j.1365-3091.1962.tb00455.x.

Bowen, B.B., Bernau, J.A., Kipnis, E.L., Lerback, J.C., Wetterlin, L., and Kleba, B., 2018a, The making of a perfect racetrack at the Bonneville Salt Flats: The Sedimentary Record, v. 16, no. 2, p. 4–11, https://doi.org/10.2110/sedred.2018.2.4.

Bowen, B.B., Kipnis, E.L., and Pechmann, J.M., 2018b, Observations of salt crust thickness change at the Bonneville Salt Flats from 2003-2016, *in* Emerman, S.H., Bowen, B.B., Simmons, S., and Schamel, S. editors, Geofluids of Utah: Utah Geological Association Publication 47, p. 247–285.

Bright, J., Kaufman, D.S., Oviatt, C.G., and Clark, D.L., 2022, Amino acid racemization geochronology results from the Wendover core in the Salduro quadrangle, Utah: Utah Geological Survey Open-File Report 741, 3 p., appendix, https://doi.org/10.34191/OFR-741.

Christiansen, J.E., and Patil, B.B., 1962, Salt Flats investigations progress report part X: Transmissibility tests – 1961, Salt Flats investigations: Utah State University Engineering Experiment Station Project EC 35. p. 87-95.

Christiansen, J.E., Thorpe, J.D., Tovey, T., and Patil, B.B., 1960a, Salt Flats investigations progress report part I—Pumping tests on Salt Flats, Salt Flats investigations: Utah State University Engineering Experiment Station Project EC 35. 46 p.

Christiansen, J.E., Thorpe, J.D., Tovey, T., Patil, B.B., and Morin, W., 1960b, Salt Flats investigations progress report part II—Pumping tests on Salt Flats, Salt Flats investigations: Utah State University Engineering Experiment Station Project EC 35. 99 p.

Clark, D.L., Oviatt, C.G., Hardwick, C.L., Langenheim, V.E., Bowen, B.B., Bernau, J.A., and Page, D., in preparation, Geologic map of the Bonneville Salt Flats and east part of the Wendover 30' x 60' quadrangles, Tooele County, Utah: Utah Geological Survey Map, scale 1:62,500.

Clark, D.L., Oviatt, C.G., Hardwick, C., and Page, D., 2020, Interim geologic map of the Bonneville Salt Flats and east part of the Wendover 30' x 60' quadrangles, Tooele County, Utah–Year 3: Utah Geological Survey Open-File Report 731, 30 p., 2 plates, scale 1:62,500, https://doi.org/10.34191/OFR-731.

Clark, D.L., Oviatt, C.G., and Page, D., 2016, Geologic map of Dugway Proving Ground and adjacent areas, Tooele County, Utah: Utah Geological Survey Map 274DM, 31 p. 2 plates, scale 1:75,000, https://ugspub.nr.utah.gov/publications/maps/m-274/m-274txt.pdf.

Eardley, A.J., 1962, Gypsum dunes and evaporite history of the Great Salt Lake Desert: Utah Geological and Mineralogical Survey Special Studies 2, https://ugspub.nr.utah.gov/publications/special_studies/SS-2.pdf.

Fitzmayer, J., Larsen, D. Braxton, D., and Staes, E., 2004, Hydrogeology of Government Creek basin, Dugway, Utah, with a recommended practical approach to ground-water management in arid, saline regions of the Great Basin, *in* Spangler, L.E. editor, Ground Water in Utah–resource, protection, and remediation: Utah Geological Association Publication 31, p. 161–178.

Forester, R.M., 1988, Nonmarine calcareous microfossil sample preparation and data acquisition procedures: U.S. Geological Survey Technical Procedure HP-78 RI, p. 1–9.

Graf, D.L., Eardley, A.J., and Shimp, N.F., 1961, A preliminary report on magnesium carbonate formation in glacial Lake Bonneville: The Journal of Geology, v. 69, no. 2, p. 219–223, https://doi.org/10.1086/626730.

Grim, R.E., Kulbicki, G., and Carozzi, A., 1960, Clay mineralogy of the sediments of the Great Salt Lake, Utah: Bulletin of the Geological Society of America, v. 71, no. April, p. 515–520, https://doi.org/10.1130/0016-7606(1960)71[515:CMOTSO]2.0.CO;2.

Hart, I., Jones, K.B., Brunelle, A., DeGraffenried, J., Oviatt, C.G., Nash, B.P., Duke, D., and Young, D.C., 2022, Building a master chronology for the western Lake Bonneville Basin with stratigraphic and elemental data from multiple sites, USA: Radiocarbon, v. 64, no.1, p. 69–85, https://doi.org/10.1017/RDC.2022.3.

Kipnis, E.L., and Bowen, B.B., 2018, Observations of salt crust change from 1960-2016 and the role of humans as geologic agents at the Bonneville Salt Flats, Utah, *in* Emerman, S.H., Bowen, B.B., Simmons, S., and Schamel, S. editors, Geofluids of Utah: Utah Geological Association Publication 47, p. 287–303.

Langford, R.P., 2003, The Holocene history of the White Sands dune field and influences on eolian deflation and playa lakes: Quaternary International, v. 104, no. 1, p. 31–39, https://doi.org/10.1016/S1040-6182(02)00133-7.

Langford, R.P., Rose, J.M., and White, D.E., 2009, Groundwater salinity as a control on development of eolian landscape—An example from the White Sands of New Mexico: Geomorphology, v. 105, no. 1–2, p. 39–49, https://doi.org/10.1016/j.geomorph.2008.01.020.

Lindenburg, G.J., 1974, Factors contributing to the variance in the brines of the Great Salt Lake Desert and the Great Salt Lake: Salt Lake City, University of Utah, M.S. thesis, 70 p.

Lines, G.C., 1979, Hydrology and surface morphology of the Bonneville Salt Flats and Pilot Valley playa, Utah: Geological Survey Water-Supply, v. 2057, no. 2057, p. 1–107, https://doi.org/10.3133/wsp2057.

Louderback, L.A., and Rhode, D.E., 2009, 15,000 years of vegetation change in the Bonneville basin—the Blue Lake pollen record: Quaternary Science Reviews, v. 28, no. 3–4, p. 308–326, https://doi.org/10.1016/j.quascirev.2008.09.027.

Madsen, D.B., Oviatt, C.G., Young, D.C., and Page, D., 2015, Chapter 3—Old River Bed delta geomorphology and chronology, *in* Madsen, D.B., Schmitt, D.N., and Page, D., editors, The Paleoarchaic occupation of the Old River Bed delta, University of Utah Anthropological Papers #128, p. 30–60.

Martin, P.S., and Mehringer, P.J., 1965, Pleistocene pollen analysis and biogeography of the Southwest, in Wright, H.E. and Frye, D.G. editors, The Quaternary of the U.S.: Princeton University Press, p. 433–451, https://doi.org/10.1515/9781400876525-026.

Mayo, A.L., Tingey, D.G., Rey, K.A., Winkel, T.D., McBride, J.H., Nelson, S.T., Carling, G.T., Bruthans, J., and Petersen, E.C., 2020, Shallow groundwater flow and inverted fresh/saline-water interface in a hypersaline endorheic basin (Great Basin, USA): Hydrogeology Journal, v. 28, no. 8, p. 2877–2902, https://doi.org/10.1007/s10040-020-02209-8.

Miller, D.M., Felger, T.J., and Langenheim, V.E., 2021, Geologic and geophysical maps of the Newfoundland Mountains and part of the adjacent Wells 30' x 60' Quadrangles, Box Elder County, Utah: Utah Geological Survey Miscellaneous Publication 173DM, 27 p., 2 plates, scale 1:62,500, https://doi.org/10.34191/MP-173DM.

Munroe, J.S., Laabs, B.J.C., Oviatt, C.G., and Jewell, P.W., 2015, Trip 1—New investigations of Pleistocene pluvial and glacial records from the northeastern Great Basin, *in* Field Trip Guidebook, Sixth International Limnogeology Congress, Reno, Nevada, June 15–19, 2015, p. 1–30, https://doi.org/10.1130/2011.0021(01).

Nackowski, M.P., 1962, Brine exploration—Bonneville Salt Flats: Bonneville Limited Drilling Program, April 1, 1961, 50 p., 1 plate.

Nielsen, D., Watkins, R.K., and Christiansen, J.E., 1962, Salt Flats investigations progress report Part VI—Physical tests on Soil Samples From Under Salt Island, Salt Flats investigations: Utah State University Engineering Experiment Station Project EC 35, p. 3–24.

Nolan, T.B., 1927, Potash brines in the Great Salt Lake Desert, Utah—Chapter B, *in* Contributions to economic geology (short papers and preliminary reports): U.S. Government Printing Office, p. 25–44, https://doi.org/10.3133/b795B.

Oviatt, C.G., 2015, Chronology of Lake Bonneville, 30,000 to 10,000 yr BP: Quaternary Science Reviews, v. 110, p. 166–171.

Oviatt, C.G., 2017, Ostracodes in Pleistocene Lake Bonneville, eastern Great Basin, North America: Hydrobiologia, v. 786, no. 1, p. 125–135, https://doi.org/10.1007/s10750-015-2483-y.

Oviatt, C.G., 2021, Geomorphic controls on sedimentation in Pleistocene Lake Bonneville, eastern Great Basin, *in* Starratt, S.W., and Rosen, M.R. editors, From saline to freshwater–the diversity of western lakes in space and time: Geological Society of America Special Paper 536, p. 53–66, https://doi.org/10.1130/SPE536.

Oviatt, C.G., Clark, D.L., Bernau, J.A., and Bowen, B.B., 2020, Data on the surficial deposits of the Great Salt Lake Desert, Bonneville Salt Flats and east part of the Wendover 30' x 60' Quadrangles, Tooele County, Utah: Utah Geological Survey Open-File Report 724, 70 p., https://doi.org/10.34191/OFR-724.

Oviatt, C.G., Habiger, G.D., and Hay, J.E., 1994, Variation in the composition of Lake Bonneville marl—a potential key to lake-level fluctuations and paleoclimate: Journal of Paleolimnology, v. 11, no. 1, p. 19–30, https://doi.org/10.1007/BF00683268.

Oviatt, C.G., Madsen, D.B., and Schmitt, D.N., 2003, Late Pleistocene and early Holocene rivers and wetlands in the Bonneville basin of western North America: Quaternary Research, v. 60, no. 2, p. 200–210, doi:10.1016/S0033-5894(03)00084-X.

Oviatt, C.G., Pigati, J.S., Madsen, D.B., Rhode, D.E., and Bright, J., 2018, Juke Box trench–a valuable archive of late Pleistocene and Holocene stratigraphy in the Bonneville basin, Utah: Utah Geological Survey Miscellaneous Publication 18-1, 15 p., https://ugspub.nr.utah.gov/publications/misc_pubs/mp-18-1.pdf.

Oviatt, C.G., Thompson, R.S., Kaufman, D.S., Bright, J., and Forester, R.M., 1999, Reinterpretation of the Burmester Core, Bonneville Basin, Utah: Quaternary Research, v. 52, no. 2, p. 180–184, https://doi.org/10.1006/qres.1999.2058.

Palacios-Fest, M.R., Duke, D., Young, D.C., Kirk, J.D., and Oviatt, C.G., 2021, A paleo-lake and wetland paleoecology associated with human use of the distal Old River Bed Delta at the Pleistocene-Holocene transition in the Bonneville Basin, Utah, USA: Quaternary Research, no. 2021, p. 75–93, doi:10.1017/qua.2021.49

Pedone, V.A., and Oviatt, C.G., 2013, South to north flow in Lake Bonneville—Evidence from carbonate mineralogy and geochemistry [abstract]: Geological Society of America Abstracts with Programs, p. 7123, https://gsa.confex.com/gsa/2013AM/webprogram/Paper224470.html.

Pedone, V.A., and Oviatt, C.G., 2016, Water chemistry changes over time and space in Lake Bonneville during the post-Stansbury transgression: *in* Oviatt, C.G. and Shroder, J.F. editors, Lake Bonneville–A Scientific Update, p. 442–461, https://doi.org/10.1016/B978-0-444-63590-7.00016-0.

R Core Team, 2021, R—A language and environment for statistical computing: R Foundation for Statistical Computing, Vienna, Austria, https://www.R-project.org/.

Reed, J.A., 2007, The paleontological stratigraphic interval construction and analysis tool: Ames, Iowa State University, M.S. thesis, 28 p.

Rey, K.A., 2012, Insights into the early transgressive history of Lake Bonneville from stratigraphic investigation of playa, Pilot Valley NV, UT: Provo, Brigham Young University, M.S. thesis, 60 p.

Rey, K.A., Mayo, A.L., Tingey, D.G., and Nelson, S.T., 2016, Late Pleistocene to early Holocene sedimentary history of the Lake Bonneville Pilot Valley embayment, Utah-Nevada, USA, *in* Oviatt, C.G. and Shroder, J.F. editors, Lake Bonneville–A Scientific Update, p. 184–220, https://doi.org/10.1016/B978-0-444-63590-7.00010-X.

Reynolds, R.L., Yount, J.C., Reheis, M., Goldstein, H.L., Chavez, P., Fulton, R.S., Whitney, J., Fuller, C.C., and Forester, R.M., 2007, Dust emission from wet and dry playas in the Mojave Desert, USA: Earth Surface Processes and Landforms, v. 34, March, p. 613–628.

Rosen, M.R., 1994, The importance of groundwater in playas—A review of playa classifications and the sedimentology and hydrology of playas: Geological Society of America Special Papers, v. 289, no. January 1994, p. 1–18.

Schnurrenberger, D., Russell, J., and Kelts, K., 2003, Classification of lacustrine sediments based on sedimentary components: Journal of Paleolimnology, v. 29, no. 2, p. 141–154, https://doi.org/10.1023/A:1023270324800.

Shuey, R.T., 1971, Paleomagnetic chronology and correlation of Great Salt Lake basin sediments: Washington D.C., National Science Foundation, Final Technical Report for grant GA-16134, 15 p.

Smith, R.P., Breckenridge, R.P., and Wood, T.R., 2012, Assessment of geothermal resource potential at a high-priority area on the Utah Testing and Training Range–South (UTTR–S): Idaho National Laboratory, prepared for the U.S. Department of Energy, Assistant Secretary for Energy Efficiency and Renewable Energy, Under DOE Idaho Operations Office, Contract DE-AC07-05ID14517, 156 p., https://inldigitallibrary.inl.gov/sites/sti/sti/5411185.pdf.

Stephens, J.C., 1974, Hydrologic reconnaissance of the northern Great Salt Lake Desert and summary hydrologic reconnaissance of northwestern Utah: Utah Geological and Mineral Survey, p. 5–24, https://waterrights.utah.gov/docSys/v920/w920/w9200094.pdf.

Turk, L.J., 1973, Hydrogeology of the Bonneville Salt Flats, Utah: Utah Geological and Mineral Survey, 82 p., https://ugspub.nr.utah.gov/publications/water_resources_bulletins/WRB-19.pdf.

Turk, L.J., Davis, S.N., and Bingham, C.P., 1973, Hydrogeology of lacustrine sediments, Bonneville Salt Flats, Utah: Economic Geology, v. 68, no. 1, p. 65–78, https://doi.org/10.2113/gsecongeo.68.1.65.

Utah Department of Transportation, 1969a, Wendover to Arinosa, T Line over I-80, Situation and Layout, Utah. Online through the Utah GeoData Archive System, https://geodata.geology.utah.gov/pages/download.php?direct=1&noattach=true&ref=6310&ext=pdf&k=, accessed November 2022.

Utah Department of Transportation, 1969b, Wendover to Arinosa, County Road Over I-80, Situation and Layout, Utah. Online through the Utah GeoData Archive System, https://geodata.geology.utah.gov/pages/download.php?direct=1&noattach=true&ref=6311&ext=pdf&k=, accessed November 2022.

Utah Division of Oil, Gas and Mining (UDOGM), 2023, Well database: Online, https://oilgas.ogm.utah.gov/oilgasweb/live-data-search/lds-well/well-main.xhtml, accessed April 6, 2023.

Utah Division of Water Rights, 2022, Water Rights Database: Online, https://www.waterrights.utah.gov/wrinfo/query.asp, accessed November 2022.

Whelan, J.A., and Petersen, C.A., 1974, Bonneville Salt Flats–A possible geothermal area?: Utah Geological and Mineral Survey Open-File Report 14,Utah Geology, v. 1, no. 1, p. 71–82. Utah Geological and Mineral Survey Open-File Report 14, 21 p., https://ugspub.nr.utah.gov/publications/open_file_reports/OFR-14.pdf.

Williams, S.K., 1994, Late Cenozoic tephrostratigraphy of deep sediment cores from the Bonneville Basin, northwest Utah: Geological Society of America Bulletin, v. 106, no. 12, p. 1517–1530.

# APPENDICES

# APPENDIX A

## Smear Slide and Ostracode Data

The figures in this appendix depict the general results of smear slide and ostracode analysis within analyzed cores and exposures. The leftmost column depicts smear-slide-based aragonite relative to other carbonate percentages. The central column depicts the occurrence of ostracode fragments and diatoms (cysts, fragments, and whole) in smear slides (note samples were not processed to concentrate diatoms). The right-most column depicts the abundance of ostracodes in samples processed for ostracodes. Appendix A figures and data are available online: https://ugspub.nr.utah.gov/publications/open_file_reports/ofr-754/ofr-754a.zip.

# APPENDIX B

## Sediment Log Data

Sediment logs for all sites are available in a tabular form online: https://ugspub.nr.utah.gov/publications/open_file_reports/ofr-754/ofr-754b.xlsx. These files are formatted for the PSICAT program (Reed, 2007) and can be used to reproduce the logs in appendix C, but they are readable as a stand-alone file.

# APPENDIX C

## Graphical Sediment Logs

Sediment logs for all described sites. Logs include interpreted chronology, where data was appropriate. Logs are divided by area and depth of investigation, with shallow logs extending from the ground surface to 15 m depth (3.3 m on average), alluvial-fan logs from the alluvial-fan area extending from the surface to 111 m depth (64 m on average), and deep logs from the GSLD extending from the surface down to 1300 m depth (450 m on average). Data from a portion of these cores is available online at: https://geology.utah.gov/apps/rockcore/index.html.

### Appendix C1: Shallow Sites

https://ugspub.nr.utah.gov/publications/open_file_reports/ofr-754/ofr-754c1.pdf

### Appendix C2: Alluvial-Fan Sites

https://ugspub.nr.utah.gov/publications/open_file_reports/ofr-754/ofr-754c2.pdf

### Appendix C3: Deep Sites

https://ugspub.nr.utah.gov/publications/open_file_reports/ofr-754/ofr-754c3.pdf